Does irrigation with reclaimed water significantly pollute shallow aquifer with nitrate and salinity? An assay in a perurban area in North Tunisia

Makram Anane · Youssef Selmi · Atef Limam · Naceur Jedidi · Salah Jellali

Abstract In Tunisia, reclaimed water is increasingly used for irrigation in order to mitigate water shortage. However, few studies have addressed the effect of such practice on the environment. Thus, we attempted in this paper to assess the impact of irrigation with reclaimed water on the nitrate content and salinity in the Nabeul shallow aquifer on the basis of satellite images and data from 53 sampled wells. Ordinary and indicator kriging were used to map the spatial variability of these groundwater chemical parameters and to locate the areas where water is suitable for drinking and irrigation. The results of this study have shown that reclaimed water is not an influential factor on groundwater contamination by nitrate and salinity. Cropping density is the main factor contributing to nitrate groundwater pollution, whereas salinity pollution is affected by a conjunction of factors such as seawater interaction and lithology. The predictive maps show that nitrate content in the groundwater ranges from 9.2 to 206 mg/L while the electric conductivity ranges from 2.2 to 8.5 dS/m. The high-nitrate concentration areas underlie sites with high annual crop density, whereas salinity decreases gradually moving away from the coastline. The probability maps reveal that almost the entire study area is unsuitable for drinking with regard to nitrate and salinity levels. Appropriate measures, such as the elaboration of codes of good agricultural practices and action programs, should be undertaken in order to prevent and/or remediate the contamination of the Nabeul shallow aquifer.

Introduction

Due to its arid and semi-arid climate, Tunisia is facing water scarcity problems, where the estimated available freshwater is only about 450 m^3/citizen/year (Louati et al. 2000). Thus, the competent institutions have regulated reclaimed water (RW) use to tackle water penury and to fulfill part of the increased demand for irrigation. Since the early 1960s, 600 ha were irrigated with RW to save the citrus trees located at Soukra (North East of Tunis city) facing an overexploitation and salinization of the groundwater. More attention has been paid to the RW within the following 30 years, having been considered as an important part of Tunisia's overall water resources balance. During this period, the irrigated area with RW has increased progressively to reach 9,555 ha in 2010. The water reuse has been diversified into other applications such as urban green spaces watering, and aquifer and wet lands recharge (Bahri 2002; ONAS 2011).

Regulation of RW use has been developed through standards and rules in order to assure the sustainability of the practice. Considerable researches related to RW irrigation have been undertaken in pilot areas of Tunisia, to assess their fertilizing value and also their

M. Anane (✉) · Y. Selmi · A. Limam · N. Jedidi · S. Jellali
Wastewater Treatment Laboratory, Water Researches and Technologies Center, Technopark Borj Cedria. Carthage University, P.B. 273, 8020 Soliman-Tunisia, Tunisia
e-mail: makram.anane@certe.rnrt.tn

contaminating effect on crops and soil (Bahri 1991; Khelil et al. 2009; Bedbabis et al. 2010; Klay et al. 2010). These researches revealed that, when appropriate measures are taken, RW contribute in increasing crops productivity compared with fresh water with insignificant contamination impact on crops and soil (Bahri 1991; Khelil et al. 2009; Bedbabis et al. 2010; Klay et al. 2010). However, when used for long time, RW may lead to groundwater pollution especially by nitrate and salinity (Abu-Zeid 1998; Salgos et al. 2006; Chen et al. 2010; Hanjra et al. 2012).

In Tunisia, no attention has been paid to the impact of RW long-term use on groundwater quality. Groundwater contamination by nitrate is a global issue as it could potentially cause health problems to humans, such as methemoglobin rate increase in blood, cancer risk, and oxygen-carrying capacity decrease (WHO 2004). As well, high content of salts in water may threaten the health and livelihood of individuals and may degrade the productivity of agricultural land when used for irrigation (Demir et al. 2009).

Monitoring and controlling the impact of long-term use of RW on groundwater allows development of strategies in order to assure its agricultural sustainable use. Set-up spatial distribution of nitrate content and salt in groundwater is an effective way for this control. It helps to understand the polluting influential factors and then to protect or/and remediate the aquifer from contamination. Besides irrigation with reclaimed water, many other sources could pollute groundwater with nitrate and salts, such as fertilizers, at-site wastewater disposal systems, sludge drying, geo-chemical weathering of rocks and parent material, irrigation return flow, and seawater intrusion (McLay et al. 2001; Babiker et al. 2004; Di et al. 2005; Van den Brink et al. 2007; Alcala and Custodio 2008; Chamtouri et al. 2008; Baba and Tayfur 2011; El Ayni et al. 2011; Lorenzen et al. 2011; Zghibi et al. 2011).

Within the last decades, geostatistics have been used worldwide to determine spatial variability of groundwater salinity and nitrate concentrations and to identify areas suitable for drinking and irrigation (Demir et al. 2009; Chen et al. 2010; Dash et al. 2010; Tutmez and Hatipolu 2010). Geostatistical methods estimate the values of a parameter of interest at unsampled locations from sparse, often expensive sampled data (Isaaks and Srivastava 1989; Burrough 2001). On the other hand, Geographic Information System (GIS) has been developed to collect and manipulate geographical data and to overlay and combine different spatial layers (Burrough

2001). GIS and geostatistics have been, nowadays, integrated in powerful packages for spatial analyses in multidisplinary studies on natural open systems (Burrough 2001; ESRI 2003; Getis 2007). Both allow the estimation of unsampled data and combination of the output layers with other spatial and descriptive data for managing and analyzing environmental phenomena and resolving ecological and natural problems (Juang et al. 2002; Goovaerts et al. 2005; Li 2010; Sollitto et al. 2010; Varouchakis et al. 2012; Varouchakis and Hristopulos 2013a, b). Geostatistics-GIS have been widely used to investigate groundwater contamination with nitrate and salinity and to identify spatial relationships with pollution sources. For instance, Andrade and Stigter (2009), Chen et al. (2010) and Al Kuisi et al. (2009) mapped the nitrate content in the groundwater of Coimbra city in Portugal, Huantai County in China, and Amman-Zarqa Basin in Jordan. They respectively associated the polluted zones to the fertilization and the quality of water used for irrigation, to the wastewater use for irrigation, and to the chemical fertilizers. As well, Karrou et al. (2010) and Zghibi et al. (2011) mapped the salinity in the groundwater of oriental coastal aquifer in Tunisia; Gassama et al. (2012) mapped them at Vanur aquifer in India, and Al Kuisi et al. (2009) mapped the salinity in the Amman-Zarqa Basin in Jordan. They respectively linked the salinity in groundwater to the seawater intrusion, to the water–rock interaction, and to the irrigation return flow.

The present study aims at testing whether the long-term use of reclaimed water for irrigation contributes significantly to contaminate the shallow aquifer with nitrate and salinity and mapping the suitability of groundwater for drinking and irrigation with regard to these parameters. The resulting maps would help engineers and decision-makers to better manage the groundwater and undertake the necessary measures for its protection and remediation. The agricultural per-urban area of Nabeul city is taken as a case study since it includes irrigated districts with reclaimed water for a long period (ONAS 1993).

Materials and methods

Study area

The study area is located at 'Cap Bon' peninsula at the North Eastern part of Tunisia and belongs to Nabeul

District (Fig. 1). It corresponds to the peri-urban area of Grand Nabeul city located between Dar Chaaban and Beni Khiar. It covers about 15 km^2 of surface area, with a length of 5 km and a width of 3.5 km. The climate is semi-arid with 400 mm as annual average precipitation at Nabeul city and 19 °C as average temperature. The altitude varies between 0 and 110 m. Geologically, the region is Pliocene and Quaternary, mainly composed by sandstones, conglomerates, and clay. The depth of the aquifer varies from 1 to 18 m. The economic activities are mainly based on rain-fed and irrigated agriculture. Rain-fed agriculture is based mainly on olive trees, whereas irrigated agriculture is much more diversified, targeting vegetables (potatoes, tomatoes, pimiento …) when groundwater is used for irrigation and citrus, olives, tobacco, and fodder when reclaimed water is used.

Two areas, Bir Romaana and Beni Khiar, covering 120 and 85 ha, are irrigated with the effluents of two wastewater treatment plants, respectively since 1984 and 1998. Due to the lack of water from dams and other sources of fresh water, the use of reclaimed water was the sole available solution to save these districts from disappearance (ONAS 1993).

Two wastewater treatment plants (WWTP), namely SE3 and SE4, are used to satisfy the districts water needs. The first WWTP uses oxidation ditches as treatment process, with a nominal flow rate of 3,500 m^3/day (Bahri 1998; ONAS 2008). The second WWTP uses mean load activated sludge and anaerobic digestion as a treatment process, with a nominal flow rate of 9,585 m^3/day (Bahri 1998; ONAS 2008). Table 1 presents the annual averaged values of the main physico-chemical and bacteriological parameters of SE3 and SE4 effluents (ONAS 1993).

Trace element concentrations are very low in the influents and effluents of both plants (ONAS personal communication, 2012). Bahri (1998) states that Fe, Zn, Pb, Mn, Cu, Ni, Cr, Co, and Cd concentrations in the SE3 and SE4 effluents are below the maximum concentrations recommended for agricultural reuse by the Tunisian standards. Currently, SE4 is under extension and rehabilitation for capacity increasing and treatment quality improvement. A tertiary process using a sand filter and UV lamp is projected (ONAS personal communication, 2012).

Data collection and physico-chemical analysis

Totally 53 groundwater samples were collected from wells in private land between April and May 2010.
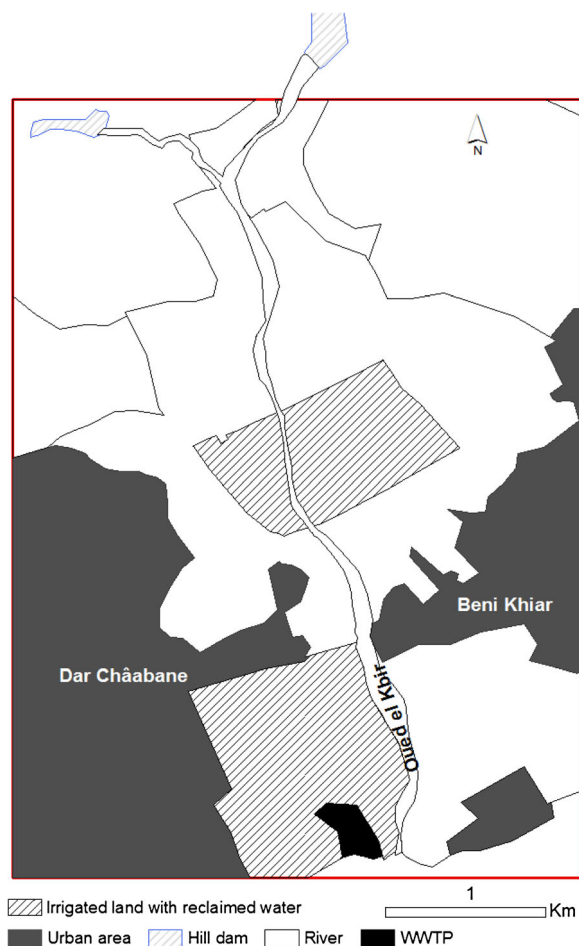

Fig. 1 Description of the study area

Table 1 Characteristics of SE3 and SE4 effluents (ONAS 1993)

	SE3	SE4
pH	7.7	7.8
EC (dS/m)	2.98	3.49
BOD$_5$ (mg/L)	14.2	24.7
COD (mg/L)	89.4	125
TSS (mg/L)	15	16
Total N (mg/L)	23	61
NH$_4$-N (mg/L)	0.03	1.8
PO$_4$ (mg/L)	4.5	5.5
K (mg/L)	47.3	71.6
Cl (mg/L)	639	678
FC (NTU/100 mL)	3.7E5	2.6E5

The selection of wells was carried out through a random-stratified sampling design in order to cover the entire study area and assure a relatively homogeneous distribution throughout the region. The process consists of dividing the study area in a mesh of grids, 500-m-side each. From each grid, one to two wells were selected randomly when available. The location of the wells was precisely recorded using a Garmin Global Positioning System receiver while the depth to water table was measured using piezometric sonde. Other data such as cropping system and land use type surrounding the well were recorded. Water temperature, pH, electric conductivity (EC), and salinity were measured in situ using WTW-type multiparameter. The samples were transfered to the laboratory in polyethylene bottles where nitrate ions (NO_3^-) concentration was measured by UV-visible spectrophotometer (Spectronic Unicam) using the salicylic method.

The piezometric head map was elaborated from the depth to water table values and altitude data obtained from the topographic map. The land use polygonal layer map was obtained through digitizing on screen the very-high-resolution satellite images supplied by GoogleEarth and through field visits and farmers consultation.

In addition, the lithology cores located inside or near the study area were collected from the "Commissariat Regional de Developpement Agricole of Nabeul" and drawn in order to describe the unsaturated and saturated zones lithology.

Descriptive statistical analysis of the data

The mean, the standard deviation (SD), and the coefficient of variation (CV) for nitrate concentration and EC were obtained. The former parameter determines the central tendency of the values and the latter two describe their variability. Normality of samples distribution was checked using Shapiro–Wilk W tests (Shapiro et al. 1968). If the W test is significant, the normality of the distribution should be then rejected. Square transformation was applied to nitrate values in order to normalize their positively skewed data set (Table 2). Furthermore, the linear regression of nitrate loads and salinity values was investigated. Then, nitrate concentration and EC were divided into intervals on the one hand, and a point symbol map showing the samples location and their respective interval was drawn, on the other hand.

Impact of reclaimed water and land use on salinity and nitrate concentration of groundwater

To check whether irrigation with reclaimed water significantly pollutes shallow aquifer with nitrate and salinity, a comparative analysis was carried out between the irrigated land with RW class, the irrigated land class with freshwater, and built-up land class.

On the other hand, an additional comparative analysis based on cultivation type was undertaken. The influence of cultivation type in GW pollution with nitrate is stated by many authors (McLay et al. 2001; Babiker et al. 2004; Di et al. 2005; Johnson and Belitz 2009). The amount of fertilizers supplied to annual crops is higher than the amount supplied to the trees resulting in a higher risk of groundwater pollution (Johnson and Belitz 2009). Consequently, the irrigated land of the study area was divided in classes according to the density of parcels with annual crops compared with the density of parcels with fruit trees. Three classes were hence defined: high density, moderate density, and low density of crops.

The physical and hydrogeological factors such as topography, hydrogeology, soil texture, lithology, and the vadose zone thickness affect the fate of nitrate and salinity and then their spatial distribution in the groundwater (Aller et al. 1987). To highlight the influence of some of these parameters, an additional comparison was carried out. This comparison is based on the subdivision of the irrigated agricultural land in units according to the irrigated water type (groundwater or reclaimed water), the density of crops compared to trees (low, moderate, and high density), and the distance to the sea which is strongly related to the depth to the groundwater table (thickness of the vadose zone).

The geographical delimitation of these classes and units was carried out based on satellite image, field visits, and consultation with farmers, the staff of regional agricultural institutions, and local irrigation organizations. Then, the sampled wells were grouped according to their location in these classes and units. Basic descriptive statistics were applied on nitrate concentration and EC for each group of samples and illustrated in a box-whisker plot for visual comparison. A statistical comparative analysis between classes and units was performed using the non-parametric Mann–Whitney U test to detect differences between the medians. The significance of this test determines the influence of reclaimed water, the significance of the cultivation type, and other

Table 2 Descriptive statistics of depth to water, electric conductivity, nitrate, and root square of nitrate of the 53 wells

	N	Min	Max	Mean	SD	CV	W-Test	P value	Skewness	Kurtosis
EC (dS/m)	53	0.6	8.5	4.6	1.8	0.39	0.99	0.98	−0.002	−0.396
NO_3^- (mg/L)	53	1.3	401.9	127.6	109.9	0.86	0.90	0.0004	0.870	0.121
SQRT (NO_3^-)	53	1.1	20.0	10.0	5.3	0.53	0.96	0.06	−0.017	−0.897

factors on groundwater pollution with nitrate and salinity.

Upscaling procedure

The upscaling procedure consisted on a spatial interpolation of nitrate content and EC from the sampled wells to the unsampled locations in order to get (1) prediction maps offering a visual representation and displaying a continuous spatial variability of these parameters throughout the GW of the study area and (2) probability maps that delineate suitable sites for drinking and irrigation. The probability maps help make the decision to prevent and/or remediate GW pollution.

Spatial statistical analysis of the data

A spatial statistical analysis was applied on nitrate and EC data in order to study their spatial dependence at global and local levels. These analyses allow checking the presence or absence of global spatial autocorrelation and identifying local patterns of spatial dependence such as outliers and clusters. The presence of a global spatial autocorrelation in a pattern is a prerequisite to interpolate the measured parameters from the sampled locations to the unvisited points and to map a continuous distribution of their values all over the study area. Spatial autocorrelation for nitrate and EC among GW samples was tested using Moran's I statistic (I) (Moran 1948). I is calculated based on feature locations and attribute values simultaneously. Its equation can be represented as follows:

$$I = \frac{n\sum_i\sum_j w_{ij}\left(x_i-\overline{x}\right)\left(x_j-\overline{x}\right)}{\sum_i\sum_j w_{ij}\sum_i\left(x_i-\overline{x}\right)\left(x_j-\overline{x}\right)^2}$$

where n is the number of sampled points, x_i and x_j are the variable values at locations i and j, $\overline{x}$ is the mean of the variable, and w_{ij} is a distance-based weight matrix which is the inverse distance between locations i and j ($1/d_{ij}$).

I is a dimensionless test that ranges from −1 and 1. The significance of the global Moran's I is tested based on their Z scores as obtained by the following equation:

$$Z = \frac{I-E(I)}{\sqrt{\text{var}(I)}}$$

where var (I) is the variance for I and E(I) is the expected I calculated as: $E(I) = -(n-1)^{-1}$

Z score states the spatial autocorrelation or randomness of the set of analyzed data. When spatial autocorrelation is assured (Z>1.95 or Z<−1.95), positive I value indicates a clustered pattern whereas negative I value indicates dispersion (ESRI 2003; Prasannakumar et al. 2011).

As for local level, the spatial outliers are the sampled points in which values are obviously different from the values of their surrounding locations, whereas the clusters are the points in which values are significantly close to the values of their neighbors (Lalor and Zhang 2001). Identification of spatial outliers is important because they could make the process of interpolation exhibit unreliable behavior and they could move away normality from data distribution (McGrath and Zhang 2003). Identification of outliers and clusters was done using Local Moran's Index (I_i), defined by Anselin (1995) as follows:

$$I_i = \frac{x-\overline{x}}{\sum_i\left(x_i-\overline{x}\right)^2}\sum_j w_{ij}\left(x_j-\overline{x}\right)$$

I_i is calculated based on feature locations of the neighboring samples and attribute values. A positive value for I_i indicates that the feature is surrounded by features with similar values (forming a spatial cluster), whereas a negative value of I_i indicates that the feature is surrounded by features with dissimilar values (producing a spatial outlier). In parallel, a score was calculated to determine the statistical significance of the Moran's index from which the decision is taken on autcorrelation

or randomness of the set of analyzed data (ESRI 2003). The inverse distance function was used to calculate the weight of each point needed for local Moran's I equation. The index result for each parameter (nitrate and EC) was visualized in a map.

Ordinary kriging interpolation

The upscaling procedure was applied using the well-known ordinary kriging method, performed in several steps. First, the measured nitrate concentration and EC were employed to calculate the experimental semivarigrams which describe the change in the measured values as a function of distance. They are computed as half the average squared difference between the components of data pairs:

$$\gamma(h) = \frac{1}{2N(h)} \sum_{i=1}^{N(h)} [(Z(x) - Z(x+h)]^2$$

where $\gamma(h)$ is the semivariance, $Z(x)$ is the regionalized variable, and $N(h)$ the number of pairs of sample data taken for a distance h.

Different theoretical semivariograms models (i.e., spherical and exponential) were fitted to the experimental one in order to determine a mathematical function relating the semivariogram values to the distance. This function provides variogram values for all distances and guarantees their uniqueness to estimate the weights essential for kriging (Isaaks and Srivastava 1989; Webster and Oliver 2007). Different lags and directions were tested to assess the impact of the distance and the isotropy on spatial distribution. The model with best goodness of fit was selected. It was identified (1) "by eye" which is the most common method used despite its subjectivity and (2) on the basis of cross-validation through six error statistics, namely the mean absolute error (MAE), the root mean square error (RMSE), the average standard error (ASE), mean standardized error (MSE), and the root mean square standardized error (RMSSE) (Evrendilek and Ertekin 2007; Varouchakis and Hristopulos 2013b). The MAE and MSE indicate the overall tendency of the model to under- or over-predict (e.g., the degree of bias) while the RMSSE assesses the adequacy of the kriging variance as an estimate of the prediction uncertainty, and the RMSE and the ASE are measures of prediction accuracy on a point-by-point basis. The best model selected is the one

which have the closest MAE and MSE to zero, the closest RMSSE to one, and RMSE and ASK as small as possible and equal to one another (Evrendilek and Ertekin 2007; Varouchakis and Hristopulos 2013b).

Sills, ranges, and nuggets were determined from the selected theorical semivarigrams. The sill is the variogram value when the measured data variation becomes independent of the distance, whereas the range is the distance corresponding to the sill value, and the nugget is the variogram value when the distance is null. The nugget effect reflects the measurement error and the short-scale variability along with unexplained and inherent variability (Burgos et al. 2006).

Once the best model was selected, the prediction of nitrate content and salinity at unknown locations was carried out using ordinary kriging method as follows:

$$Z(X_0) = \mu + \varepsilon(X_0)$$
$$Z(X_0) = \sum \lambda_i \gamma(x_i) \quad \sum \lambda_i = 1$$

where μ is an unknown constant and $\varepsilon(X_0)$ is the error associated with an unknown location X_0, $Z(X_0)$ is the estimated value of Z at X_0, and λ_i is the weight that gives the best possible estimation from the surrounding points.

Then, the prediction maps were obtained providing visual displays of the spatial variability of nitrate content and EC throughout the groundwater of the study area. Besides, the standard error map was derived in order to illustrate the error related to the prediction of the analyzed parameters.

Mapping of GW suitability for drinking and irrigation

For decision-making point of view, it is not so important to estimate the nitrate content or salinity at unknown locations, rather than the determinination of the probability to exceed a risky value for human being or for certain use in order to take measures for remediation. Indeed, water with high nitrate content is risky for the human health, and at certain level of salinity, water used for irrigation could affect cultivation growth and deteriorate the soil when applied long-term. So it is important to map GW suitability for drinking and irrigation according to nitrate and salinity through probability maps for exceeding critical risky thresholds. Such map can be combined with expert knowledge for decision making (Goovaerts 1999). Indicator kriging is a geostatistical method best suited for this kind of issues (Isaaks and

Srivastava 1989; Webster and Oliver 2007; Goovaerts 1999). It is computed as a binary function (0 or 1) through the use of cut-off value for continuous data:

$$I(s) = \mu + \varepsilon(s)$$

$$I(s) = \begin{cases} 1 & \text{if } Z(x) \leq Z' \\ 0 & \text{otherwise} \end{cases}$$

where μ is an unknown constant, $\varepsilon(s)$ is the error associated with an unknown location, and $I(s)$ is a binary variable. $Z(x)$ is the measured value, and Z' is the cut-off value.

Since the indicator variables are 0 or 1, the interpolation is between 0 and 1, and the resulting map shows the probabilities of exceeding (or being below) the threshold (Isaaks and Srivastava 1989).

Isaaks and Srivastava (1989) state that, for most practical problems that require indicator techniques, a careful consideration of the final goal allows the use of well-chosen threshold which have a special significance to the problem being addressed. In our case, there are typically cutoff values that have specific significance for human health and crop production. Two thresholds were selected for nitrate and two for salinity. As for nitrate, the first threshold is 13 mg/L corresponding to the human affected value. Human affected value is defined as the lowest nitrate concentration indicative of natural groundwater contamination due to human activities (McLay et al. 2001; Babiker et al. 2004; Andrade and Stritger 2009). The second cut-off value is 45 mg/L which is the maximum permissible concentration of nitrate used for potable water according to Tunisian standards. As for salinity, the first threshold is 2.5 dS/m corresponding to the permissible limit for drinking recommended by World Health Organisation (WHO 2004). The second cutoff value is 4.9 dS/m corresponding to the water salinity tolerance with 90 % yield potential of barley forage (Ayers and Westcot 1985) which is one of the most tolerant cultivation in the study area.

Experimental semivariograms parameters were calculated for groundwater EC and square root nitrate concentration from the 53 sampled data. The best-fitting theoretical semivariograms selected and the corresponding semivariogram parameters were extracted. Then, the indicator kriging was applied to generate the probability of not exceedance maps for groundwater EC and nitrate content based on the threshold values previously identified.

Results and discussion

Descriptive statistical analysis of the data

Descriptive statistics of nitrate and EC of the 53 groundwater samples are presented in Table 2. Nitrate values range from 1 to 402 mg/L with a mean of 128 mg/L, which is above the maximum acceptable level according to Tunisian water quality standards for drinking (45 mg/L). Eighty-four percent of the water samples exceed the human affected value of 13 mg/L, reflecting the anthropogenical origin of nitrate. The source could be multifold resulting from inorganic fertilization and manure, irrigation with reclaimed water, leaching of animal wastes from farms, and leakage from sewers. The nitrate concentration of more than 55 % of the sampled wells exceeds 100 mg/L. Consequently, the use of this water for drinking compromises human health, and it is hence mandatory to take measures to prevent the potential risks on citizens.

On the other hand, EC values range from 0.6 to 8.5 dS/m with a mean of 4.6 dS/m, which is above the permissible limit (2.5 dS/m) recommended by WHO (2004). More than 10 % of the wells have salinity lower than 2.5 dS/m. However, only 4 % have a very good water quality (<1.5 dS/m) while more than 43 % of wells have high salinity levels exceeding 4.9 dS/m. The low salinity could be attributed to the surface water recharge from the Oued el Kbir crossing the area from the north to the South. The high salinity is the consequence of a conjunction of factors including dissolution of minerals from evaporite rocks, irrigation return flow, leaching of minerals to GW released from organic and inorganic fertilizers, seawater intrusion, and infiltration of sea-salt spray to GW by rainwater (Ben Moussa et al. 2011a, b; Ben Hamouda et al. 2011).
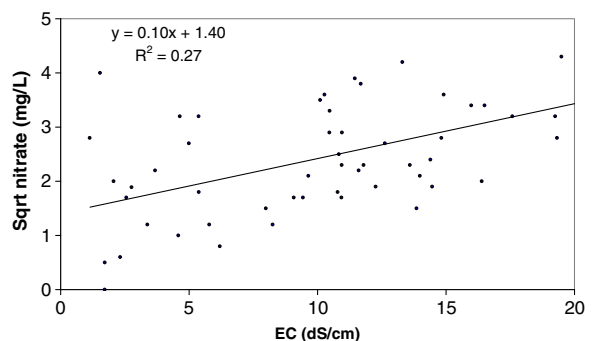

Fig. 2 Linear regression analysis of nitrate and salinity values

The coefficient of variation of nitrate is 0.86 which is less than the half of EC one (0.38). This difference is linked to the importance of external factors (fertilization, quality of irrigated water …) influencing the nitrate pollution distribution compared with salinity. Shapiro–Wilk W test reveals that EC values follow a normal distribution however nitrate does not. The nitrate data have a long tail towards higher concentration because of the relatively smaller percentage of high values. The probability distribution is positively skewed (skewness=0.87) while the skewness of salinity is almost zero (−0.02). The normality of nitrate set of data is obtained applying a square root transformation. This transformation made the set of data much closer to normality and a skewness almost zero (−0.01).

As regards the regression analysis carried out on the 53 sampled wells between EC and root square nitrate content, it shows an influence of nitrogen fertilizer on GW salinity (Fig. 2). This relationship enhances a significant linear relationship ($P<0.01$; intercept=1.4; slope=0.10; $r=$ 0.52). However, this relationship is weak, being 27 % of EC variability due to nitrate content.

Concerning the point symbol mapping of nitrate, Fig. 3a illustrates the distribution of sampled wells according to nitrate concentrations intervals ranging respectively from 0–13, 13–45, 45–200, and >200 mg/L. The high values are clustered in two main areas, one located in the south and the other in the center east. The low values are grouped in areas close to the river, one in the center and the other in the north. Figure 3b presents the point symbol map of EC illustrating the distribution of sampled EC values into the intervals 0–1.1, 1.1–2.5, 2.5–4.9, and >4.9 dS/m. The low values go alongside the river bed which stresses the natural aquifer recharge with good-quality surface water. The high values are observed mostly in the south near the coastline, stressing the influence of seawater in the
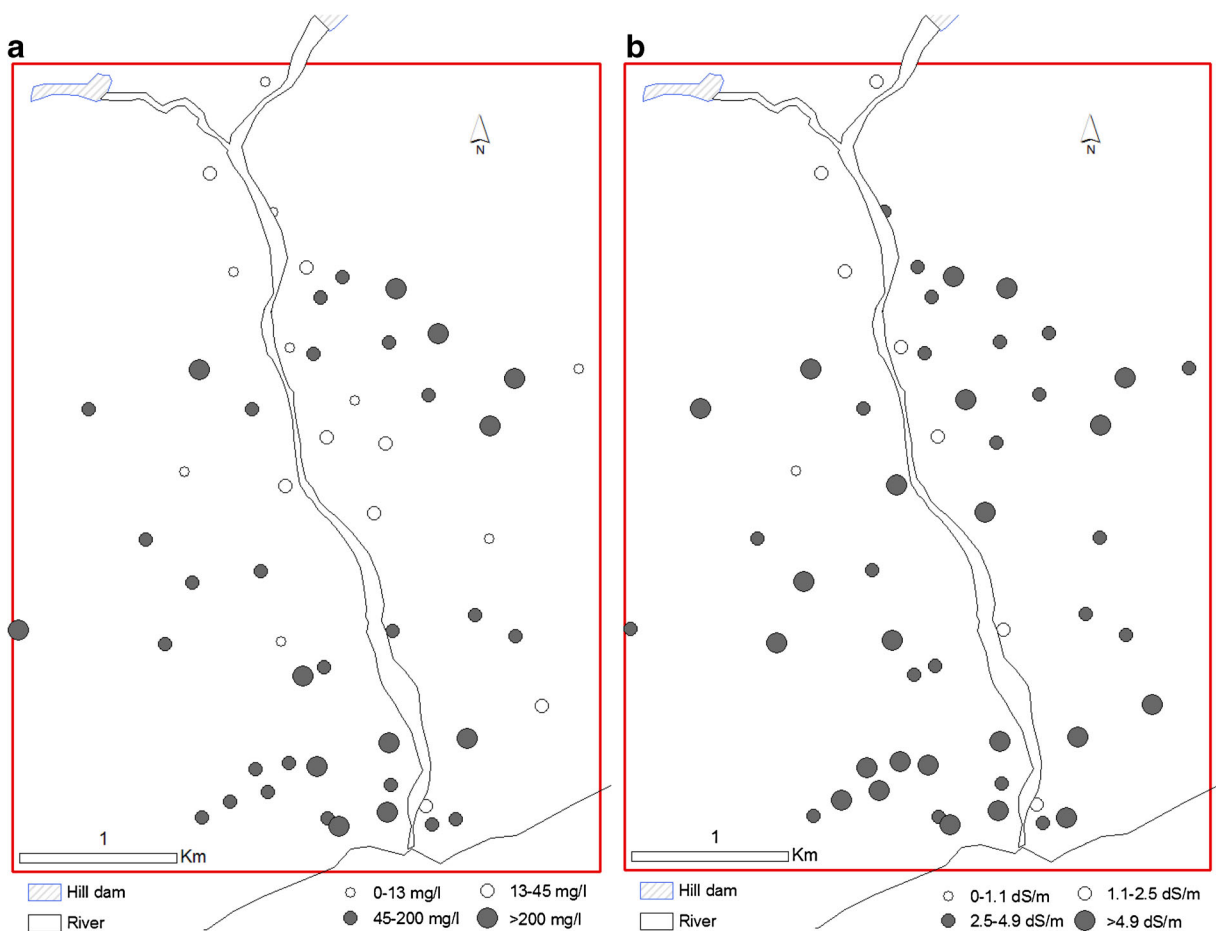
Fig. 3 Point symbol map of **a** nitrate and **b** electric conductivity

salinization of GW through salt spray or seawater intrusion. Due to the high salinity of groundwater, unsuitable for large varieties of crops and trees, 120 ha close to the coastline have been allocated for irrigation with reclaimed water in 1984 to safeguard the irrigated district and the farmers' quality of life.

Impact of reclaimed water and land use on salinity and nitrate concentration of groundwater

The land use map obtained from satellite images, field visit, and consultation with farmers and experts is presented in Fig. 4. It includes the different land use units as above-defined, along with the piezometric map and the sampled wells location.

The groundwater level mapping shows a N–S flow direction, from the hill dams to the natural discharge
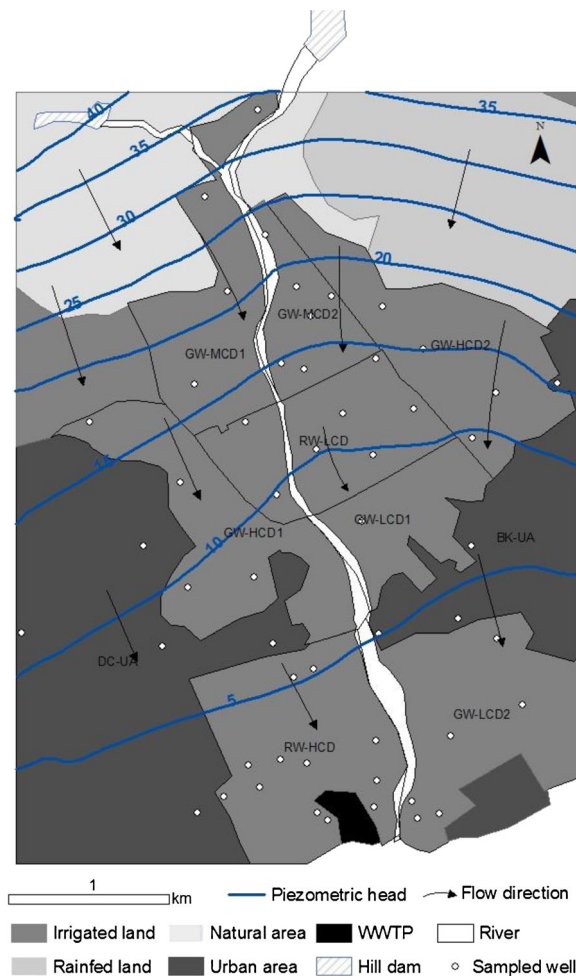
Fig. 4 Land use and piezometric maps with the sampled wells location

area of Hammamet Gulf sea. The main land uses in the area are irrigated land (775 ha), urban area (421 ha, natural vegetation (180 ha), rain-fed area (180 ha), and WWTP (7.5 ha). No appropriate well responding to the objectives of this study has been found in the last three land uses. Therefore, the statistical analysis concerning this section has been done only for urban and irrigated areas. The number of sampled wells of each land use, class, and unit along with the mean of nitrate content and EC are presented in Table 3. The box-and-whisker plot for each class and unit is presented in Fig. 5.

The study area is segregated in ten units (Table 3) as follows:

– Two units irrigated with reclaimed water, one of which with low crop density (RW-LCD) and the other with high crop density (RW-H CD);
– Six units irrigated with groundwater, from which two irrigated units with low crop density (GW-LCD), two with medium crop density (GW-MCD), and two with high crop density (GW-HCD); and
– Two units located in urban areas, one in Beni Khiar (BK-UA) and the other one in Dar Chaabane (DC-UA).

Nitrate

Mann–Whitney U test reveals no significant differences in GW nitrate concentration between the irrigated land with RW, the irrigated land with freshwater, and the urban area (Table 4). The mean of these three classes is around 120 mg/L. These results point out that irrigation with RW does not significantly influence groundwater contamination with nitrate. Indeed, the SE3 and SE4 effluents are richer in ammonium than in nitrate (Table 1). Ammoniacal nitrogen contained in wastewater is quickly adsorbed by soils colloidal through caption exchange capacity. Over time, only small part of the adsorbed ammonium by soils colloidal could be nitrified and lesser nitrate is lost by leaching towards groundwater. In fact, the nitric nitrogen (very soluble in water) is the only nitrogen compound that can migrate with water through soil and subsoil layers without adsorption (Serhal et al. 2009). These results do not match with those given by Chen et al. (2010) and Bouri et al. (2008), which stated that irrigation with wastewater significantly affect the nitrate content in groundwater,

Table 3 The number of sampled wells of each land use, class, and unit along with the mean of nitrate content and electric conductivity

	Subgroup1	Subgoup2	Units	Area	Samples n°	Mean nitrate	Mean EC
Urban area	UA	UA		42.1	9	100.29	4.12
			DC-UA	29.7	5	126.17	4.77
			BK-UA	10.7	4	67.94	3.32
Irrigated area				77.6	44	133.16	4.46
	GW-Irr			20.9	25	124.57	4.47
	RW-Irr			56.5	19	144.4-	5.12
		Low crop density (LCD)		25.9	14	79.31	4.84
		Moderate crop density (MCD)		13.6	10	71.83	3.36
		High crop density (HCD)		38.0	20	201.52	5.40
			RW-LCD	8.7	7	47.76	4.29
			RW-HCD	12.2	12	200.9	5.61
			GW-LCD1	5.4	1	21.5	5.93
			GW-LCD2	11.6	6	125.8	5.29
			GW-MCD1	9.0	4	66.6	2.59
			GW-MCD2	4.6	6	75.3	3.87
			GW-HCD1	10.1	4	81.6	4.38
			GW-HCD2	10.4	4	323.4	5.77

in Huantai County (China) and Sidi Abid Region (Tunisia), respectively. The wastewater used for Chen et al. (2010) is untreated sewage contrary to the secondary treated wastewater used in Nabeul per-urban area. Bouri et al. (2008) did not compare irrigated area with reclaimed water to irrigated lands with freshwater but with rain-fed agricultural land.

Urban area is highly contaminated with nitrate revealing no significant difference between this class and the irrigated land classes. The operating septic tanks still installed in many houses and the city sewage network leakages could be the reason of the GW contamination with nitrate. Similar deductions have been reported by Chamtouri et al. (2008) who showed that the GW is highly polluted under Sfax city (Centre of Tunisia) because of pit latrine and recharge wells installed before the sewage network settlement.

Mann–Whitney U test carried out between the high density of crops, the medium density of crops, and the low density of crops reveals that the high-density class is significantly different from the two others (Table 5), with a much higher median, which indicates that the density of annual crops significantly affects the nitrate content in the underlying GW. The annual crops of the study area are mainly market gardening and fodder. Synthetic fertilizers rich in nitrogen compounds, such

as ammonitrate (NH_4NO_3), di-ammonium phosphate (DAP) ((NH_4)$_2$$HPO_4$), nitrate of potassium, and nitrate of calcium, are provided to these crops much heavily than any other land uses. Indeed, in the study area, an average of 10 quintals per hectare of chemical fertilizers is supplied to the annual crops and less than 3 quintals to citrus and fruit trees. An important part of the nitrate released in the soil is leached to groundwater, boosted by the traditional gravity irrigation commonly adopted and the crop shallow roots systems. In addition, in the per-urban area of Nabeul, it is common to plant crops twice a year, which increases the amount of fertilizers released and raises the nitrate leachate to groundwater (Di and Cameron 2002). Groundwater nitrate pollution attributed to market gardening is pointed out in several studies around the word (McLay et al. 2001; Mohamed et al. 2003; Andrade and Stigter 2009; Chen et al. 2010). On the other hand, groundwater nitrate content is low where the proportion of permanent fruit trees is high because (1) the fertilization of the fruit trees is provided mainly as manure, from where mineral nitrogen transformation is relatively slow and gradual, (2) the low frequency of irrigation that does not exceed four times a year, and (3) the developed and deep root system of the trees are able to assimilate nitrate from the upmost soil horizon to the deepest. Changes in the type of
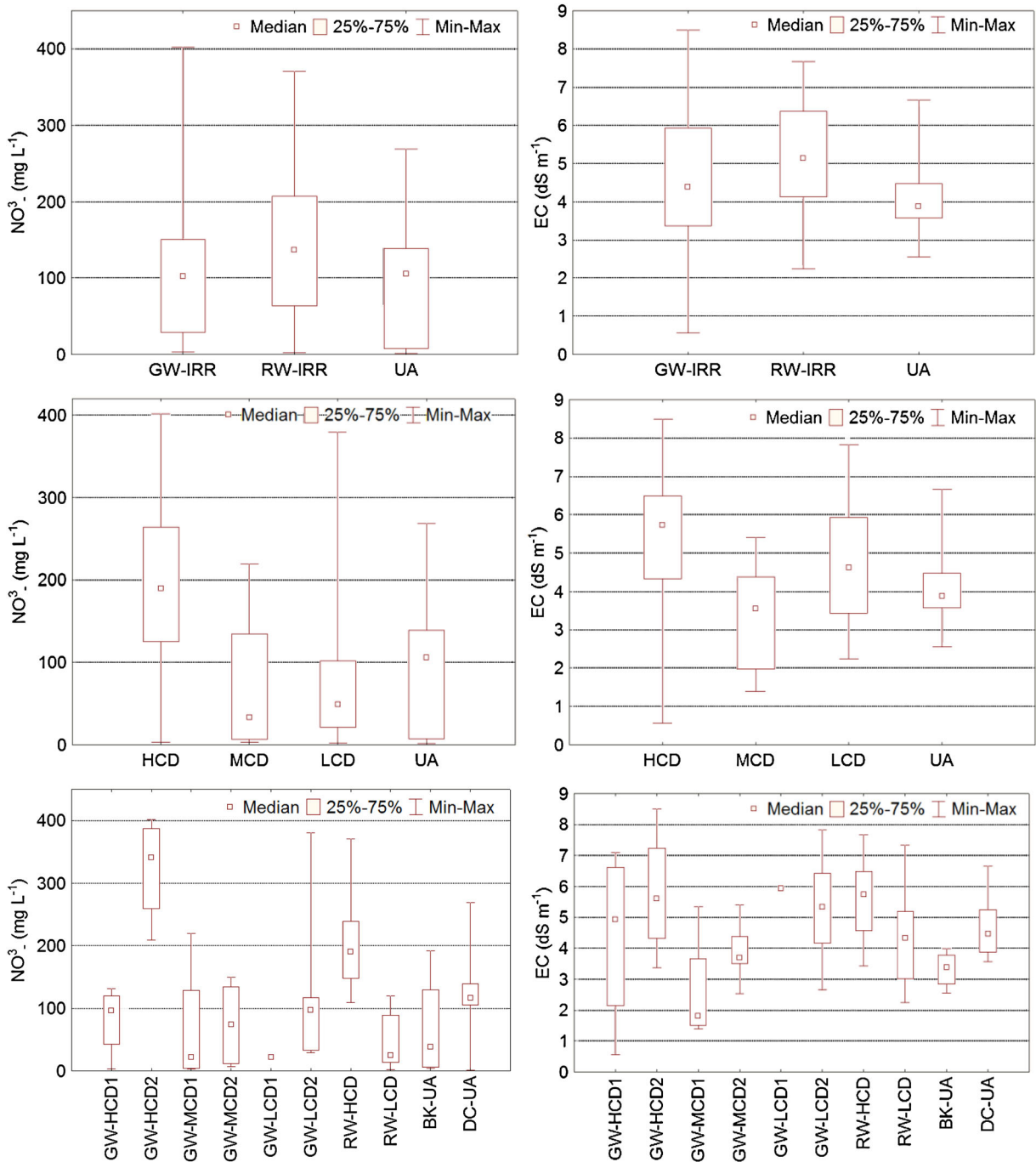
Fig. 5 Box-and-whisker plot for each land use class and unit for nitrate and electric conductivity data

cultivation from crops to trees could tackle and remediate the problem of contamination with nitrate if soil and social conditions are appropriate. This was stated by Chen et al. (2010), who have pointed out that, under the same irrigation conditions in Huantai County in China, shallow groundwater nitrate concentration has decreased when the land use had been changed from crops to trees.

Land use strongly affects nitrate concentration in the groundwater, but it is not necessarily the sole

Table 4 Mann–Whitney U test for nitrate median comparison between the classes: irrigated land with RW, irrigated land with freshwater and urban area

	Irrigated land with freshwater	Irrigated land with RW
Irrigated land with RW	$P>0.05$ (0.34)	
Urban area	$P>0.05$ (0.66)	$P>0.05$ (0.22)

influencing factor (Chen et al. 2010). The segregation of land use into units with respect to both water irrigation and cultivation types is helpful to detect intra-group differences. A general look to the comparison analysis between the ten segregated units with U-test (Table 6) reveals that only the units GW-HCD2 and RW-HCD differentiate significantly from the others. Three points to highlight according to these results:

- These two units (GW-HCD2 and RW-HCD) are characterized by a high density of annual crops, which corroborate what aforementioned that the high density of crops is the main cause of contamination;
- One of these two units (RW-HCD) is irrigated with reclaimed water, and it is significantly different from the other unit irrigated with reclaimed water (RW-LCD). This difference confirms that the RW is not the main influential factor for GW nitrate concentration but the density of crops;
- These two units (GW-HCD2 and RW-HCD) characterized by a high density of annual crops differentiate significantly one from the other and with a third unit characterized with a high density of crops as well (GW-HCD1). GW-HCD1 is located at the center west of the study area with the lowest nitrate concentration median (82 mgL^{-1}); GW-HCD2 is located at North East of the area with the highest median (323 mg/L), and RW-HCD is located in the

south at the coast with an in-between median (201 mg/L). This points out that, even though the main important factor for groundwater contamination is the density of crops, other factors have an impact on groundwater pollution. In this study, we were able to highlight three factors influencing the nitrate content in groundwater, namely the quality of water for irrigation, the soil texture, and the depth to water table. The influence of these factors is explained hereafter:

- *Quality of water for irrigation*: Groundwater used to irrigate GW-HCD2 unit is more concentrated with nitrate than the reclaimed water and the groundwater in GW-HCD unit. Using groundwater with high nitrate content for irrigation increases in turn the groundwater concentration with nitrate. The impact of this groundwater recycling process on the increase of nitrate content is stated by Spalding et al. (2001) and Stigter et al. (2006). A way to reduce the very high nitrate contamination in GW-HCD2 unit is to irrigate the crops with the harvested surface water in a hill dam 1 km upstream. In this respect, Stigter et al. (2006) state that the shift of irrigation from groundwater to surface water has an almost immediate effect in the upper aquifers, leading to a decrease of groundwater nitrate concentration.
- *Soil texture and unsaturated zone lithology*: The soil texture and the lithology of the unsaturated zone are different from one site to another (Farez 2008; Mariez 2008), which contribute to this difference (Fig. 6).
- *Depth to water table*: The influence of depth to water table is pointed out applying a regression analysis between root square of nitrate concentration and depth to water table measured in each sampled well. The regression analysis shows that there is a statistically significant ($P<0.05$) linear

Table 5 Mann–Whitney U test for nitrate median comparison between the classes: low density of crops, moderate density of crops, high density of crops, and urban area

	Low density of crops	Moderate density of crops	High density of crops
Moderate density of crops	$P>0.05$ (0.98)		
High density of crops	$P<0.05$ (0.001)	$P<0.05$ (0.006)	
Urban area	$P>0.05$ (0.63)	$P>0.05$ (0.29)	$P<0.05$ (0.04)

Table 6 Mann–Whitney U test for nitrate median comparison between the ten land use units

|	GW-LCD2	GW-HCD2	GW-MCD2	GW-LCD1	GW-MCD1	GW-HCD1	RW-LCD	RW-HCD	BK-UA
GW-HCD2	P>0.05 (0.07)								
GW-MCD2	P>0.05 (0.81)	P<0.05 (0.01)							
GW-LCD1	—	—	—						
GW-MCD1	P>0.05 (0.33)	P>0.05 (0.06)	P>0.05 (0.59)	—					
GW-HCD1	P>0.05 (0.91)	P<0.05 (0.03)	P>0.05 (0.74)	—	P>0.05 (0.88)				
RW-LCD	P>0.05 (0.10)	P<0.05 (0.01)	P>0.05 (0.43)	—	P>0.05 (0.92)	P>0.05 (0.40)			
RW-HCD	P<0.05 (0.03)	P<0.05 (0.02)	P<0.05 (0.007)	—	P>0.05 (0.06)	P<0.05 (0.01)	P<0.05 (0.00)		
BK-UA	P>0.05 (0.33)	P<0.05 (0.03)	P>0.05 (0.74)	—	P>0.05 (0.88)	P>0.05 (0.88)	P>0.05 (0.92)	P<0.05 (0.03)	
DC-UA	P>0.05 (0.65)	P<0.05 (0.04)	P>0.05 (0.78)	—	P>0.05 (0.54)	P>0.05 (0.54)	P>0.05 (0.19)	P>0.05 (0.10)	P>0.05 (0.54)

relationship between both parameters (intercept= 14.54; slope=−0.54). However, this relationship remains relatively weak (r=−0.37), being about 14 % of nitrate concentration variability explained by depth to water (r^2=13.9 %) (Fig. 7).

Salinity

Mann–Whitney U test reveals no significant differences of groundwater salinity between irrigated lands with RW and GW (Table 7). The mean of the two groups is around 4.5 dS/cm. Thus, water used for irrigation, whether coming from WWTPs effluents or from shallow aquifer, does not significantly influence groundwater salinity. Based on U test as well, crop density with respect to trees does not significantly influence groundwater salinity (Table 8) since the moderate crop density group differentiates significantly with low- and high-density ones, whereas these latter groups are not significantly different from one the other (Table 8). The contribution to GW salinization of more chemical compounds of the fertilizers (P, K, Zn, etc.) along with minerals dissolved from evaporite rocks renders the crop density not significantly influential for spatial variability of groundwater salinity. Ben Hamouda et al. (2011) and Ben Moussa et al. (2011a, b) state that water return flow of irrigation and the dissolution of minerals (chlorides, sulfates, and carbonates) from evaporite rocks (halite, gypsum, anhydrite, and dolomite) are important causes of Nabeul-Hammamet and Eastern Coast groundwater salinization.

The application of U test on the 10 units is presented in Table 9. This test does not show a significant difference between the most units excepting the RW-HCD one, which differentiates significantly to GW-MCD1, GW-MCD2, and BK-UA (Table 9). RW-HCD is a unit irrigated with RW and located at the south, in the coast. The excessive pumping of groundwater for irrigation contributed to shallow aquifer salinization consequence of the interaction with the seawater. To prevent the lost of long-established agricultural activities in this unit, a decision was taken in the 1980s to irrigate with the effluent of the SE4 WWTP. GW-MCD1 and GW-MCD2 units are located in the extreme north, near the hill dam and the river. These structures recharge groundwater with water harvested from the surface with very low salinity content contributing to maintaining the groundwater with good quality. The influence of
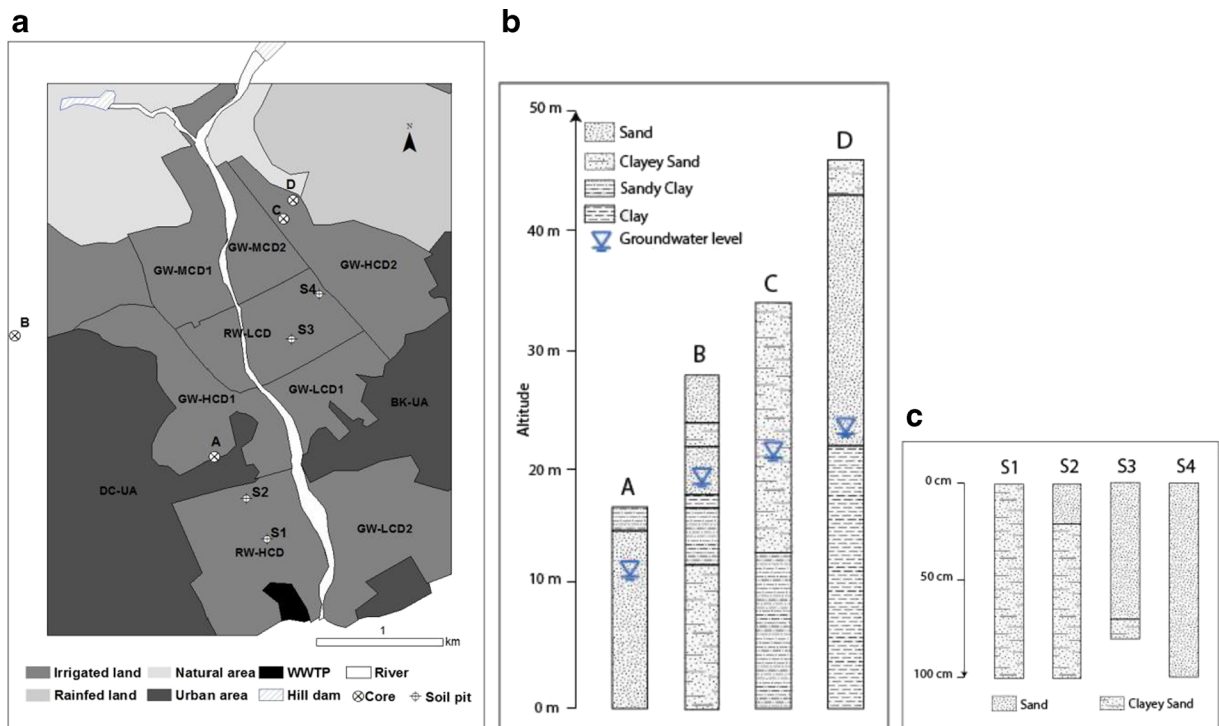
Fig. 6 **a** Location of cores and soil pits, **b** indicative lithology of the cores, **c** soil type of the soil pits

seawater on groundwater salinity is checked through a regression analysis applied between the EC and the distance of the samples from the coastline. Statistically significant ($P<0.01$) negative linear relationship (intercept=5.78; slope=−0.001; r=−0.14) is found. The regression analysis shows that about 17 % of EC variability (R^2=17.21 %) is related to the distance to seawater. Generally speaking, close areas to the sea line present higher groundwater salt content. This could be explained by two natural phenomena such as seawater intrusion and infiltration of sprayed salt by rain. These

Fig. 7 Linear regression analysis between depth to water and nitrate
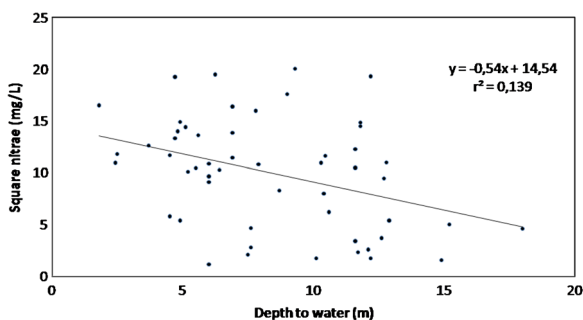
results are in concordance with Ben Hamouda et al. (2011) who state that salinity in Eastern Coast aquifer is due partially to the proximity of the sea. However, other factors such as geology and anthropological behavior also influence EC variability. A detailed composition of GW salts is required in order to identify the causes of such spatial variation.

Upscaling procedure

Spatial statistical analysis of the data

The global Moran's I for nitrate, EC, and root square nitrate indicates the presence of a significant global spatial autocorrelation (Z=2.11; 2.09 and 2.77, respectively) with clustered pattern (I=0.04; 0.04 and 0.05, respectively). The spatial relationship established allows the interpolation of the measured parameters from the sampled points over all the study area. Since normality distribution is preferred to get predictive maps, the normal-transformed square nitrate values were used rather than the originals.

The cluster and outlier analyses using local Moran's I_i reveal that 7 of 53 square nitrate samples are

Table 7 Mann–Whitney U test for electric conductivity median comparison between the classes: irrigated land with RW, irrigated land with freshwater, and urban area

	Irrigated land with freshwater	Irrigated land with RW
Irrigated land with RW	$P > 0.05$ (0.29)	
Urban area	$P > 0.05$ (0.61)	$P > 0.05$ (0.10)

significantly clustered and three are outliers (Fig. 8a). The clusters are distributed in three major regions. The first one, located at the extreme north, is characterized by a low concentration, due to surface water recharge from the river and from the hill dam. The second, located at the center, is a low–low cluster and results from the surface water recharge from the river. The third is located in the south of the area with high–high cluster. These high values are mainly the consequence of an intense supply of synthetic fertilizers. The outliers are the consequence of their location in units different from the neighbors' (Fig. 8a). Hence, two outliers have values higher than their neighbors while the third has a lower value.

The local Moran's I_i carried out for the EC reveals that eight points are significantly clustered. Four of them, characterized by high salinity, are located in the south some meters from the sea while the others, with low salinity, are located in the extreme north of the region (Fig. 8b). The former is due to an excessive pumping of groundwater along with seawater influence (salt spread and sea intrusion), and the latter is the consequence of an aquifer recharge with surface water from the hill dam and from the river. On the other hand, only one outlier is observed, located just in the center of the study area. It is a high-salinity outlier surrounded by many low salinity points. The most part of these low salinity points are located near the river, which feeds the aquifer with very good surface water quality.

The presence of more outliers for nitrate than EC suggests a higher spatial local dependence consequence of a higher impact of local man-made contamination. Even these outliers could influence negatively the interpolation; their presence is related to real phenomenon and has to be considered in the interpolation. The spatial autocorrelation proved previously and the normal distribution of the data (square nitrate and EC) make the use of interpolation appropriate and lead to accurate prediction results.

Ordinary kriging interpolation

The parameters of the best fitted theoretical semivariogram used for modeling spatial autocorrelation for nitrate and EC and the corresponding cross-validation errors are summarized in Table 10.

The nitrate experimental variogram is best fitted to a spherical model with 1,536 m range, 29 mg L^{-1} sill, and 15.6 mg L^{-1} nugget (Fig. 9). The nugget-to-sill ratio is 53 % which means a moderate spatial dependence of nitrate concentration according to Cambardella et al. (1994). Indeed, these authors quote that the variable is considered to have a strong spatial dependence if the nugget-to-sill ratio is <25 %, whereas it is moderately spatially dependent if this ratio is between 25 % and 75 %, and there is a weak spatial dependence if the ratio is >75 %. The variables which are strongly spatially dependent may be controlled by intrinsic variations, while weak spatial dependence may indicate that variability is controlled more by extrinsic variations (Sadeghi et al. 2006). Consequently, the spatial variation of nitrate in this study is affected by both extrinsic (fertilizers input) and intrinsic factors (soil texture and depth to water). There is no evident anisotropy in the variograms of nitrate which means that the concentration varies similarly in all directions and the semivariance depends only on the distance between samples (Trangmar et al. 1985).

Table 8 Mann–Whitney U test for electric conductivity median comparison between the classes: low density of crops, moderate density of crops, high density of crops, and urban area

	Low density of crops	Moderate density of crops	High density of crops
Moderate density of crops	$P > 0.05$ (0.06)		
High density of crops	$P > 0.05$ (0.27)	$P < 0.05$ (0.006)	
Urban area	$P > 0.05$ (0.32)	$P > 0.05$ (0.77)	$P < 0.05$ (0.02)

Table 9 Mann–Whitney U test for electric conductivity median comparison between the ten land use units

|	GW-LCD2	GW-HCD2	GW-MCD2	GW-LCD1	GW-MCD1	GW-HCD1	RW-LCD	RW-HCD	BK-UA
GW-HCD2	P>0.05 (0.74)								
GW-MCD2	P>0.05 (0.12)	P>0.05 (0.24)							
GW-LCD1	—	—	—						
GW-MCD1	P>0.05 (0.06)	P>0.05 (0.11)	P>0.05 (0.16)	—					
GW-HCD1	P>0.05 (0.74)	P>0.05 (0.88)	P>0.05 (0.59)	—	P>0.05 (0.47)				
RW-LCD	P>0.05 (0.35)	P>0.05 (0.22)	P>0.05 (0.94)	—	P>0.05 (0.16)	P>0.05 (0.92)			
RW-HCD	P>0.05 (0.81)	P>0.05 (0.95)	P<0.05 (0.02)	—	P<0.05 (0.02)	P>0.05 (0.50)	P>0.05 (0.08)		
BK-UA	P>0.05 (0.07)	P>0.05 (0.11)	P>0.05 (0.52)	—	P>0.05 (0.31)	P>0.05 (0.47)	P<0.05 (0.009)	P<0.05 (0.03)	
DC-UA	P>0.05 (0.65)	P>0.05 (0.62)	P>0.05 (0.24)	—	P>0.05 (0.17)	P>0.05 (0.90)	P>0.05 (0.11)	P>0.05 (0.10)	P>0.05 (0.11)

On the other hand, the EC experimental variogram is best fitted to an exponential model with a range of 4,179 m, a sill of 3.5 dS/m, and a nugget of 2.1 dS/m. The nugget-to-fill ratio is of 59 %. The ratio is between 50 % and 75 % which indicates that EC distribution has a moderate spatial dependence. Contrary to nitrate, EC presents anisotropy in the variogram, manifested by a south–north direction. The EC larger range than the nitrate indicates that the spatial variation of the salinity is more continuous and more related to natural factors while the short-range structure for nitrate suggests more man-made impact on local contamination. That was stated by Goovaerts (1999) who finds that Ni concentrations in the soil seem to vary more continuously than Cd concentrations, as illustrated by the larger range of its semivariogram. This author shows that the long-range structure of the semivariogram of Ni concentrations is probably related to the control asserted by rock type, while the short-range structure for cadmium is caused by the local man-made contamination.

The prediction maps using these spherical and exponential semivariogram models show that nitrate across the area ranges from 9.2 to 206 mg/L while salinity ranges from 2.2 to 8.5 dS/m (Figs. 10 and 11). These intervals are lower than the measured values because of the smoothing effect inherent in ordinary kriging in which large values are usually underestimated while small values are overestimated (Yamamoto 2005; Dash et al. 2010).

The spatial distribution of nitrate concentration in the groundwater predicted using ordinary kriging coincides closely with the limits of the land use units and confirms what has been obtained based on the abovementioned measured values. The presence of the most severe contamination in the units RW-HCD and GW-HCD2 as well as the lowest contamination in the GW-MCD1 and GW-MCD2 units are highlighted in the nitrate prediction map. As for salinity, the prediction map shows what has been found out using the sampled values, the gradual and continuous variation of salinity from the south sea line to the north area.

Mapping of GW suitability for drinking and irrigation

The parameters of the best-fitted theoretical semivariograms used for modelling spatial autocorrelation for nitrate and EC cut-offs, along with the corresponding cross-validation errors, are summarized in Table 11.
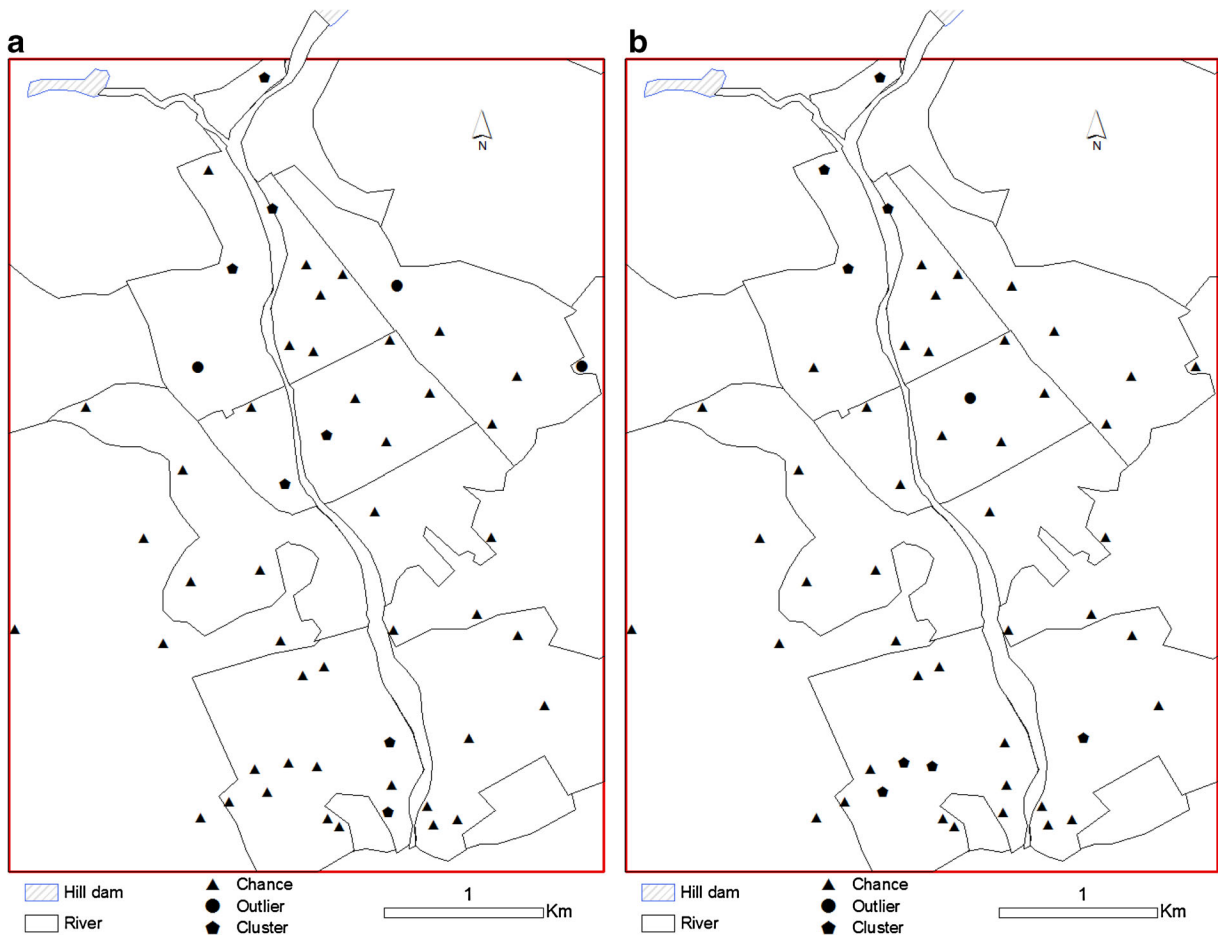
Fig. 8 Local Moran's I_i applied on the set of data of **a** nitrate and **b** electric conductivity

The nitrate experimental variograms for both cut-offs (13 and 45 mg/L) are best fitted to spherical models (Fig. 12). The range of 13 mg/L is 4,430 m while the one of 45 mg/L is 1,195 m. This difference points out that spatial variability is more continuous for the first threshold, whereas it is more small-scaled for the second one. Indeed, the very low nitrate content is registered mainly in the samples located in the half north part of the study area while, for the 45 mg/L range, it extends to the south up to the coast line (Fig. 3). This distribution influences

as well the isotropy of the variograms, being anisotropic for the lowest cut-off with north–south direction and isotropic for 45 mg/L.

The probability map reveals a quasi-absent area that does not exceed the threshold 13 mg/L (Fig. 13a). This reflects the human involvement through their agricultural activity in groundwater contamination with nitrate over almost all the shallow aquifer. Only a very small area located in the extreme north, close to the river and the hill dam, is saved. Note that this area is outside the

Table 10 Summary of best-fit models for ordinary kriging of groundwater salinity and nitrate concentration

	Model	Isotropy	AR	N	S	N/S	R	MAE	RMSE	ASE	MSE	RMSSE
Nitrate	Sph	–	–	15.64	29.46	53 %	1,536	0.000	5.04	4.80	−0.004	1.03
EC	Expon	S-N	1.00	2.10	3.55	59 %	4,179	−0.001	1.72	1.66	−0.003	1.04

AR Anisotropy ratio, *N* nugget, *S* sill, *R* range, *MAE* mean absolute error, *RMSE* root mean square error, *ASE* average standard error, *MSE* mean standardized error, *RMSSE* root mean square standardized error
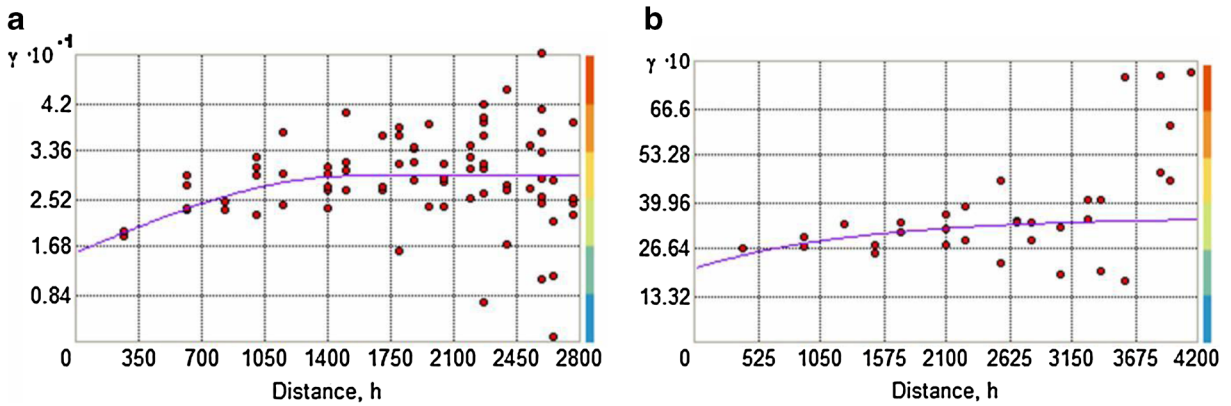
Fig. 9 Semivariograms of ordinary kriging for **a** nitrate and **b** salinity

sampled points rectangle limits where the error of prediction is too high.

The probability map not exceeding the threshold 45 mg/L, which is the permissible limit for water

drinking demanded by Tunisia law, is presented in Fig. 13b. Two clustered regions have high probability of not exceeding this limit. The first is located in the north side of the region and partly corresponds to the
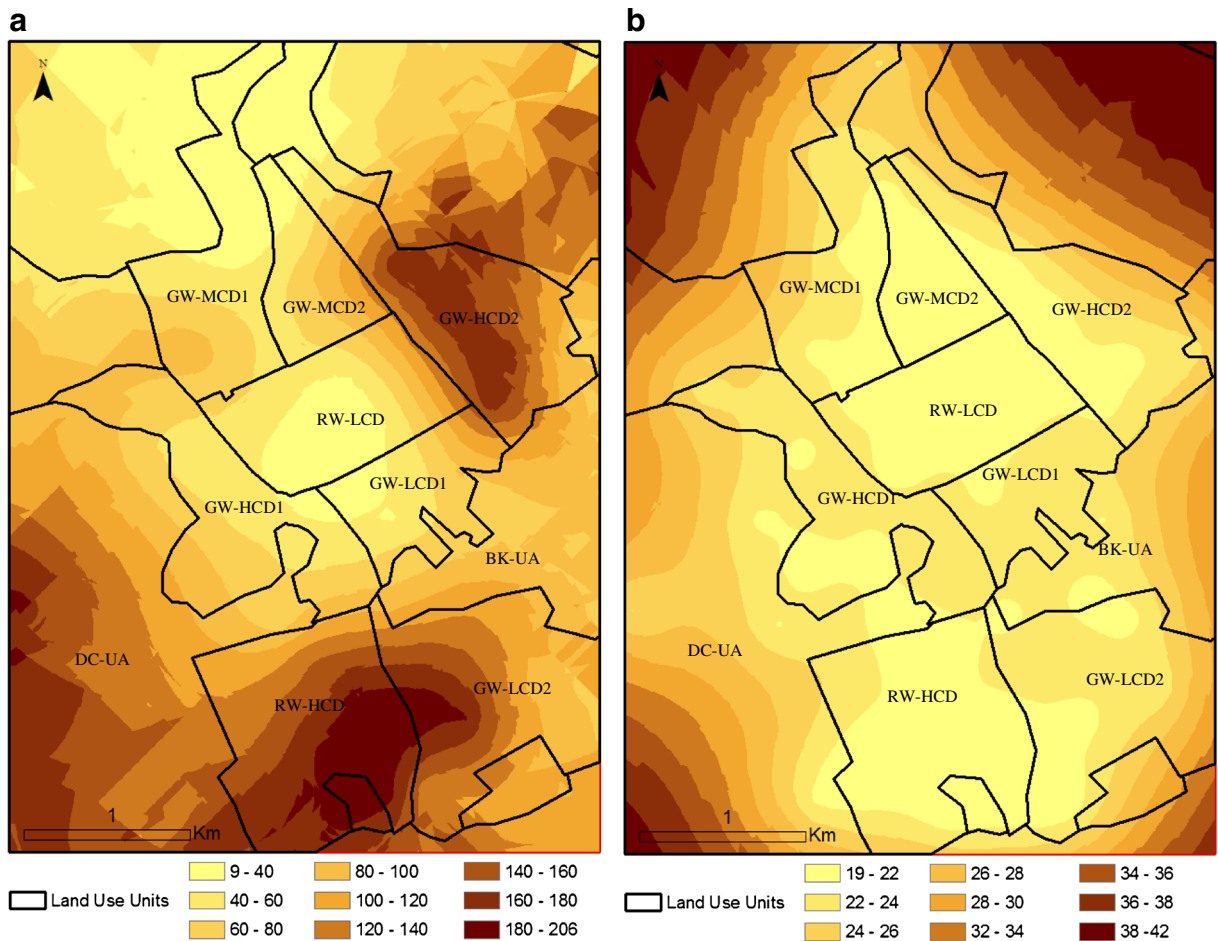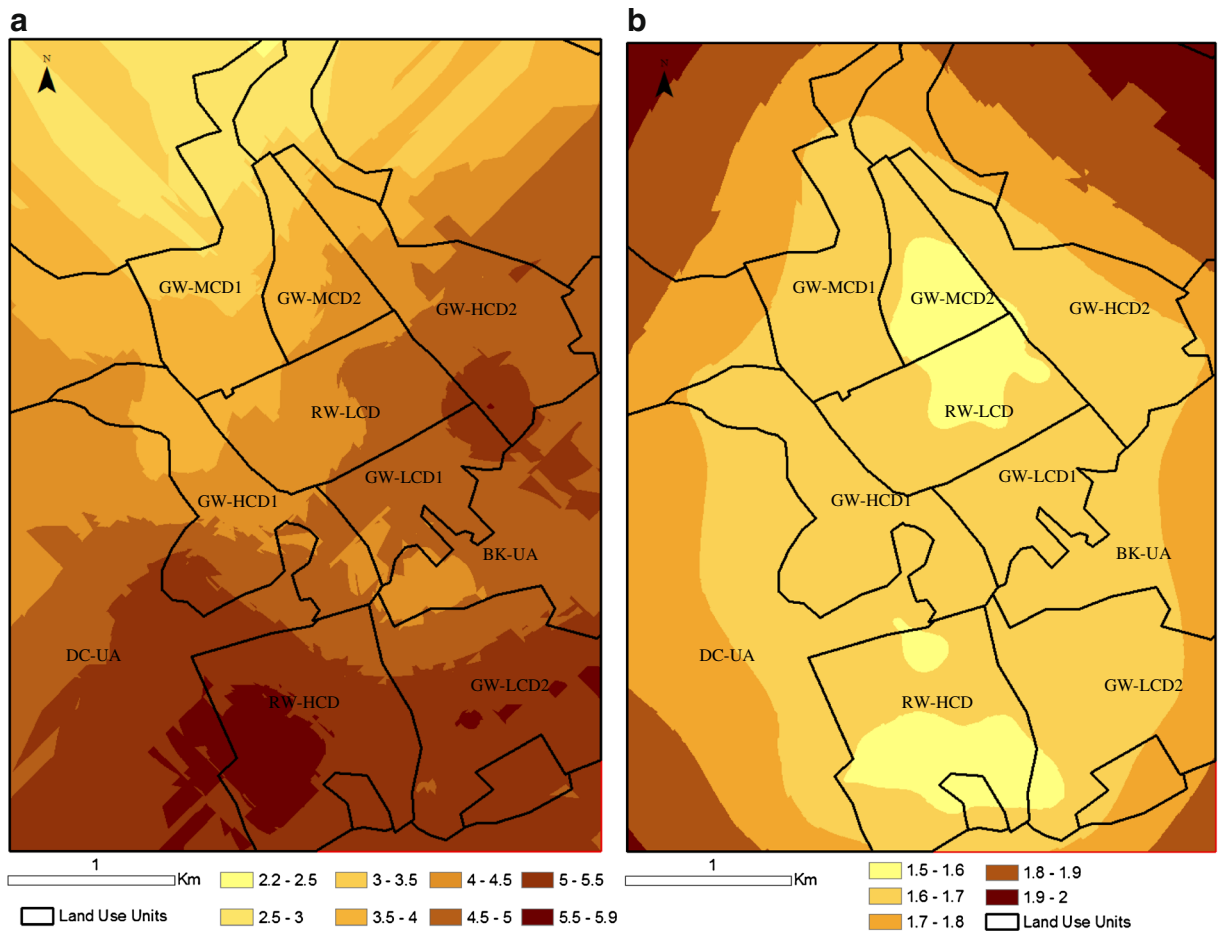

Fig. 10 Prediction map of nitrate using **a** ordinary kriging and **b** the corresponding prediction error

Fig. 11 Prediction map of electric conductivity using ordinary kriging (**a**) and the corresponding prediction error (**b**)

unaffected area by human activities. It is an area with narrow cultivated land which continually receives good quality freshwater from the surface. The second part is located in the center of the study area at the Oued el Kbir river side where citrus orchards are widespread. Excepting these two regions, the groundwater underlying the most extended area is characterized by a very low probability of being potable. Using this

groundwater wells for drinking is health risky. Hence, it is mandatory to inform the inhabitants about the threats of such practice for them to take measures to prevent its occasional use for drinking. This water under residential area should be used for other domestic purposes such as cleaning and garden watering. It is furthermore important to take effective measures against contamination produced by nitrates due to agricultural

Table 11 Summary of best-fit models for indicator kriging of groundwater salinity and nitrate concentration

|	Model	Isotropy	AR	N	S	N/S	R	MAE	RMSE	ASE	MSE	RMSSE
Nitrate (<13 mg/L)	Sph	S–N	1.00	0.10	0.17	59 %	4,430	−0.001	0.38	0.35	−0.006	1.08
Nitrate (<45 mg/L)	Sph	–	–	0.10	0.22	45 %	1,195	0.003	0.43	0.42	0.001	1.03
EC (<2.5 dS/m)	Exp	S–N	0.95	0.04	0.12	33 %	4,483	0.003	0.27	0.24	0.005	1.14
EC (<4.9 dS/m)	Exp	SE–NW	0.42	0.23	0.26	88 %	2,045	0.000	0.51	0.51	−0.003	1.00

AR anisotropy ratio, *N* nugget, *S* sill, *R* range, *MAE* mean absolute error, *RMSE* root mean square error, *ASE* average standard error, *MSE* mean standardized error, *RMSSE* root mean square standardized error
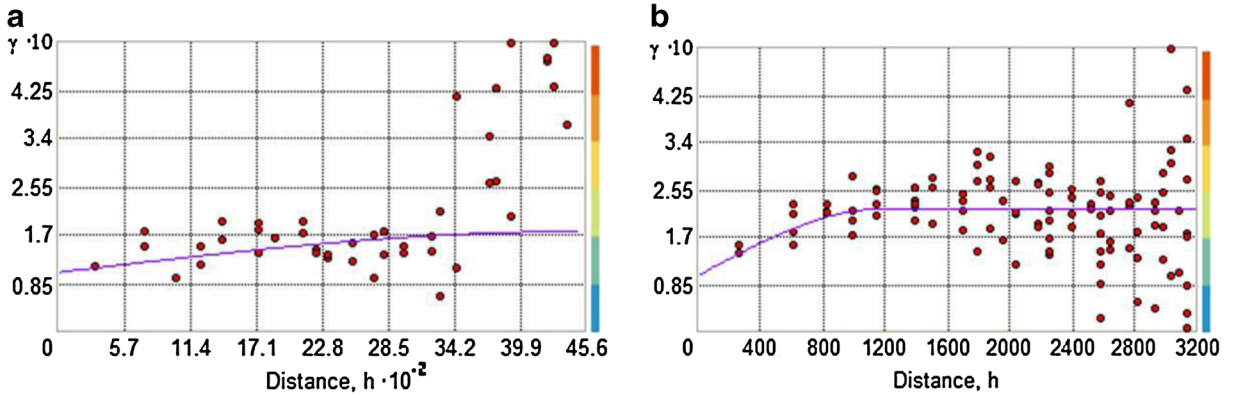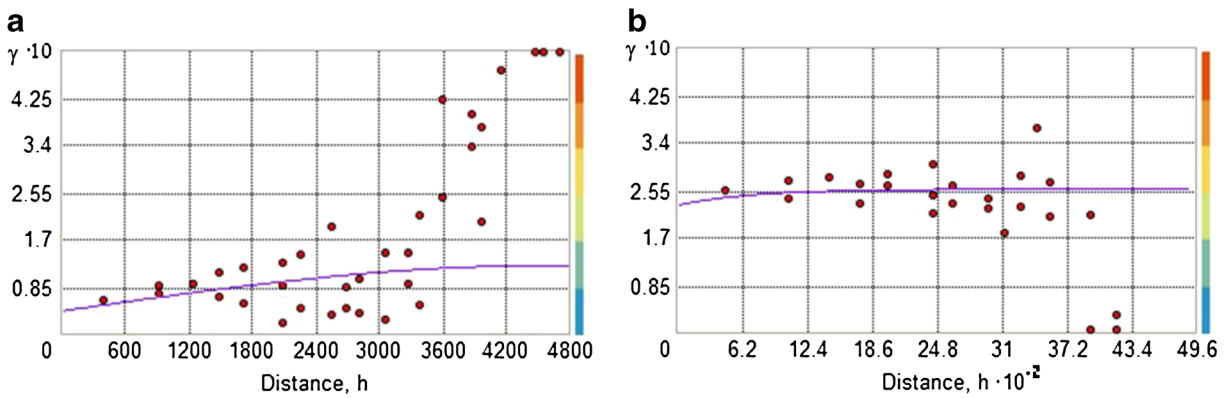
Fig. 12 Semivariograms of indicator kriging for nitrate the cut-off 13 mg/L (**a**) and 45 mg/L (**b**)

activities by elaboration of agrarian codes of good practice, actions programs, and identification and delimitation of vulnerable areas.

As for salinity, the EC experimental variograms are best fitted to exponential models for the thresholds 2.5 and 4.9 dS/m (Fig. 14; Table 11). The relative nugget is
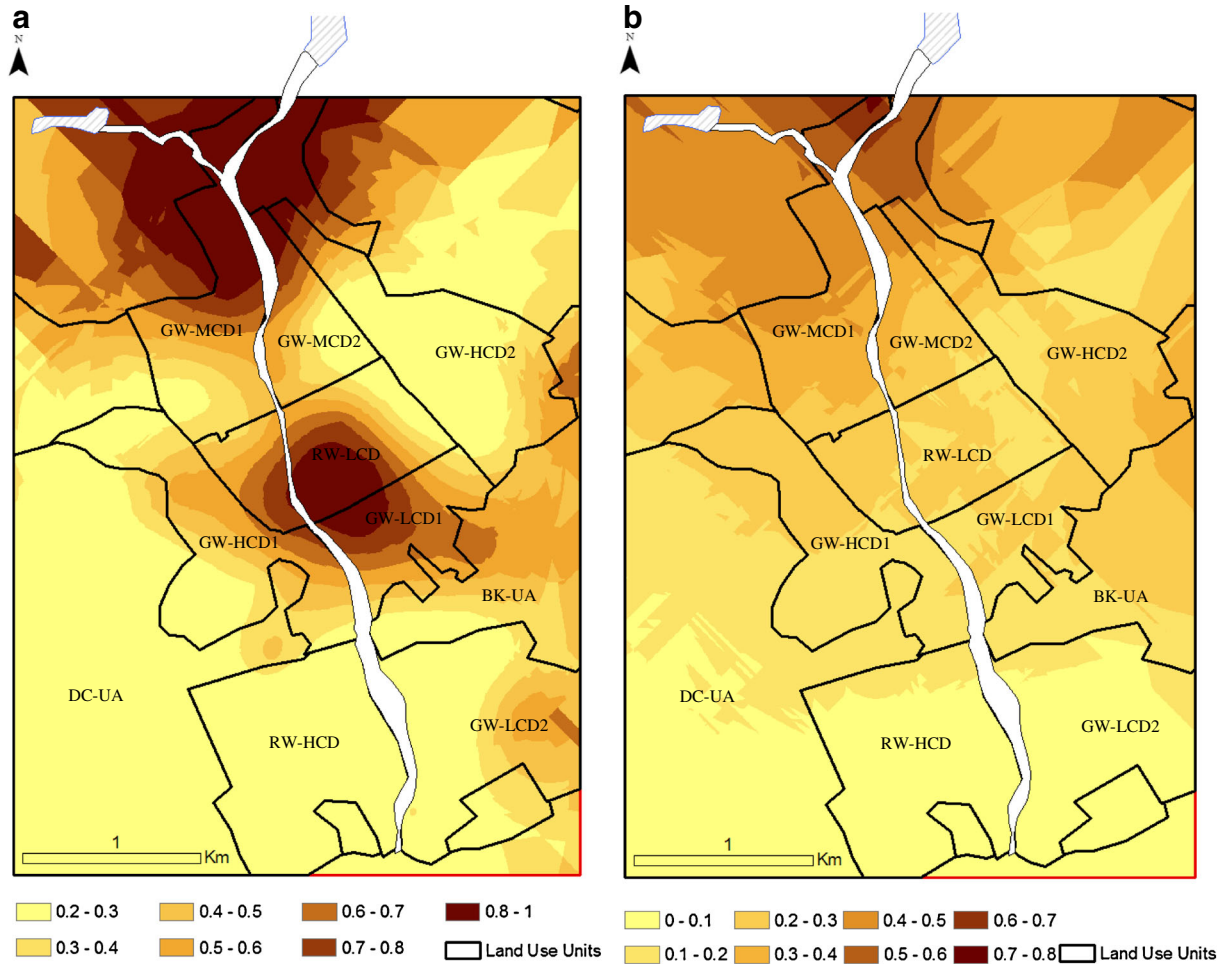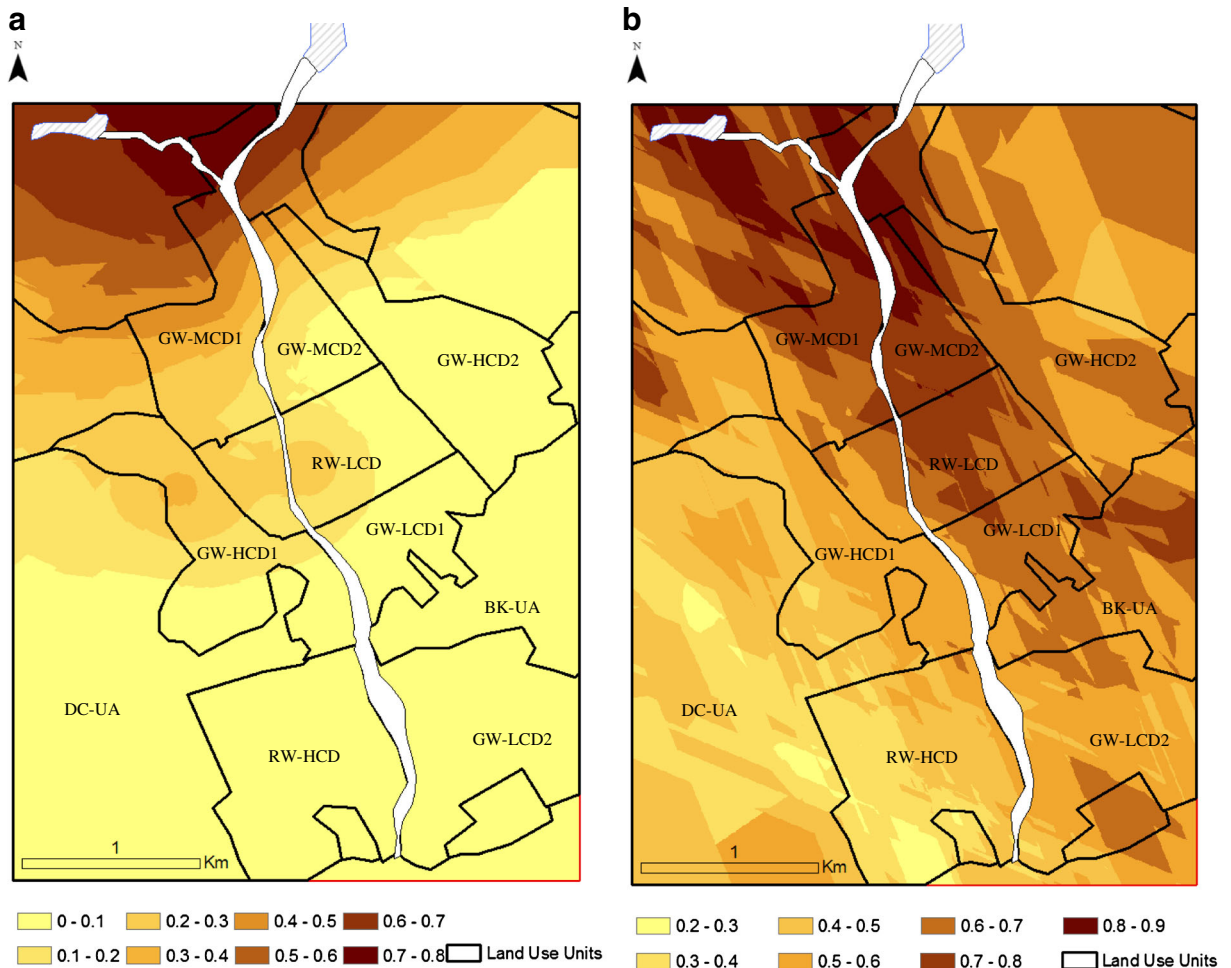

Fig. 13 Probability map using indicator kriging for the nitrate threshold of **a** 13 mg/L and **b** 45 mg/L

Fig. 14 Semivariograms of indicator kriging for nitrate the cut-off **a** 2.5 dS/cm and **b** 4.9 dS/cm

low (33 %) for the 2.5 cutoff showing a moderate spatial dependence, whereas it is high (88 %) for 4.9, indicating a weak spatial dependence. The range is higher for 2.5

revealing a higher continuous variability. These characteristics are the consequence of the spatial distribution of the samples under 2.5 and 4.9 dS/m values. For the

Fig. 15 Probability map using indicator kriging for the electric conductivity threshold of **a** 2.5 dS/m and **b** 4.5 dS/m

former, the samples are located mainly in the half north part of the study area; however, for the latter, they extend from the north to the south, up to coast line (Fig. 3).

The probability map according to 2.5 dS/m threshold reveals that the GW quality appropriate for drinking required by World Health Organisation is enclosed in a very small part of the study area. This area is located in the extreme north close to the river and a hill dam that are continually recharging the aquifer with new freshwater (Fig. 15a). The groundwater underlying the most extended area is characterized by a very low probability to be potable, including the residential area. Besides its unsuitability according to nitrate content aforementioned, groundwater under residential area is not potable according to salinity. This further stresses the risk on human health of using this water for drinking.

The area with very high probability not exceeding 4.9 dS/m is much more extended (Fig. 15b). It occupies the major part of the half north of the study area, following the river course. It covers mostly the GW-MCD1, GW-MCD2, RW-LCD, and GW-LCD1 units. Note that this threshold is an extreme salinity value not tolerated by most of crops and trees. This indicates the risk to use the groundwater for irrigation in the south part. A conjunctive irrigation with this water, reclaimed water, and good-quality surface water harvested in the hill dam has to be considered and well-studied to improve the efficiency of water use and to increase the land productivity, especially in the south part of the study area.

Conclusions

The shallow aquifer of the per-urban area of Nabeul city is clearly contaminated by nitrate, and a great part is affected by salinity. However, irrigation with reclaimed water does not influence its content with these two parameters. This corroborates the consideration of reclaimed water as opportunity to tackle water scarcity in Tunisia. It is thus recommended to be used more extensively for irrigation after taking the appropriate social and sanitary measures.

The polluted area with nitrate predicted with ordinary kriging are located mainly in two areas characterized with high density of crops, whereas the less polluted areas are located where the citrus orchards are widespread and where the irrigated land is narrow, following

the river course. The salinity prediction map shows a clear and continuous increase of salinity from the north near the coastline to the south. This spatial distribution stresses the influence of seawater in groundwater salinization through salt spray and/or seawater intrusion.

The probability maps identified the risky areas for human health and for cultivations and provided maps that could assist engineers and decision-makers to better manage the area for groundwater pollution prevention and remediation. Furthermore, an important part of the groundwater has a low probability to be potable according to nitrate content and salinity, including areas under the residential areas. Appropriate measures should be taken in order to avoid the human health risk through inhabitants' awareness on the threats of drinking such water. On the other hand, the groundwater at the southern part of the study area presents a low probability to be appropriate to irrigate sensitive cultivations to salinity. Irrigating continuously with this water could reduce the agricultural productivity and even damage the crops and the soil. Selection of tolerant crops to salinity along with a conjunctive use of groundwater with other better-quality types of water (reclaimed water and surface water) is an effective way to tackle the negative impact of groundwater use. Also, installation of drainage system could be a way to reduce groundwater salinization through reducing the irrigation return flow.

References

Abu-Zeid, K. M. (1998). Recent trends and developments: Reuse of wastewater in agriculture. *Management of Environmental Quality, 9*, 79–89.

Aller, L., Bennet, T., Lehr, J. H., Petty, R. J., & Hackett, G. (1987). DRASTIC: A standardized system for evaluating groundwater pollution potential using hydrogeological settings. US Environmental Protection Agency, EPA/600/2-87-036.

Alcala, F. J., & Custodio, E. (2008). Using the Cl/Br ratio as a tracer to identify the origin of salinity in aquifers in Spain and Portugal. *Journal of Hydrology, 359*, 189–207.

Al Kuisi, M., Al-Qinna, M., Margane, M., & Aljazzar, A. T. (2009). Spatial assessment of salinity and nitrate pollution in Amman Zarqa Basin: A case study. *Environmental Earth Sciences, 59*, 117–129.

Andrade, A. I. A. S. S., & Stigter, T. Y. (2009). Multi-method assessment of nitrate and pesticide contamination in shallow alluvial groundwater as a function of hydrogeological setting and land use. *Agricultural Water Management, 96*, 1751–1765.

Anselin, L. (1995). Local indicators of spatial association—LISA. *Geographical Analysis, 27*, 93–115.

Ayers, R. S., & Westcot, D. W. (1985). Water quality for agriculture FAO irrigation and drainage paper. Food and Agriculture Organization of the United Nations Rome, http://www.fao.org/DOCREP/003/T0234E/T0234E03.htm [last access April 2012]

Baba, A., & Tayfur, G. (2011). Groundwater contamination and its effect on health in Turkey. *Environmental Monitoring and Assessment, 183*, 77–94.

Babiker, I. S., Mohamed, M. A., Terao, H., Kato, K., & Ohta, K. (2004). Assessment of groundwater contamination by nitrate leaching from intensive vegetable cultivation using geographical information system. *Environmental International, 29*, 1009–1017.

Bahri, A. (1998). Fertilizing value and polluting load of reclaimed water in Tunisia. *Water Research, 32*, 3484–3489.

Bahri, A. (1991). L'Experience Tunisienne: en Matiere d'utilisation des Eaux Usees Traiees dans l'Agriculture. Resultats acquis et Perspectives de Recherche. Congres Mondial des Ressources en Eau. 13–18 Mai l991 . Rabat-Maroc.

Bahri, A. (2002). Water reuse in Tunisia: Stakes and prospects. In: Vers une maîtrise des impacts environnementaux de l'irrigation. Actes de l'atelier du PCSI, 28–29 mai 2002, Montpellier, France.

Bedbabis, S., Ferrarab, G., Ben Rouinac, B., & Boukhris, M. (2010). Effects of irrigation with treated wastewater on olive tree growth, yield and leaf mineral elements at short term. *Scientia Horticulturae, 126*, 345–350.

Ben Hamouda, M. F., Tarhouni, J., Leduc, C., & Zouari, K. (2011). Understanding the origin of salinization of the Plio-Quaternary eastern coastal aquifer of Cap Bon (Tunisia) using geochemical and isotope investigations. *Environmental Earth Sciences, 63*, 889–901.

Ben Moussa, A., Bel Haj Salem, S., Zouari, K., Marc, V., & Jlassi, F. (2011a). Investigation of groundwater mineralization in the Hammamet–Nabeul unconfined aquifer, north-eastern Tunisia: Geochemical and isotopic approach. *Environmental Earth Sciences, 62*, 1287–1300.

Ben Moussa, A., Zouari, K., & Marc, V. (2011b). Hydrochemical and isotope evidence of groundwater salinization processes on the coastal plain of Hammamet–Nabeul, north-eastern Tunisia. *Physics and Chemistry of the Earth, 36*, 167–178.

Bouri, S., Abida, H., & Khanfir, H. (2008). Impacts of wastewater irrigation in arid and semi arid regions: Case of Sidi Abid region, Tunisia. *Environmental Geology, 53*, 1421–1432.

Burgos, P., Madejon, E., Perez-de-Mora, A., & Cabrera, F. (2006). Spatial variability of the chemical characteristics of a trace-element contaminated soil before and after remediation. *Geoderma, 130*, 157–175.

Burrough, P. A. (2001). GIS and geostatistics: Essential partners for spatial analysis. *Environmental and Ecological Statistics, 8*, 361–377.

Cambardella, C. A., Moorman, A. T., Novak, J. M., Parkin, T. B., Karlen, D. L., Turco, R. F., et al. (1994). Field-scale variability of soil properties in central Iowa soils. *Soil Science Society of America Journal, 58*, 1501–1511.

Chamtouri, I., Abida, H., Khanfir, H., & Bouri, S. (2008). Impacts of at-site wastewater disposal systems on the groundwater aquifer in arid regions: Case of Sfax City, Southern Tunisia. *Environmental Geology, 55*, 1123–1133.

Chen, S., Wenliang, W., Hu, K., & Li, W. (2010). The effect of land use changes and irrigation water resources on nitrate contamination in shallow groundwater at county scale. *Ecological Complexity, 7*, 131–138.

Dash, J. P., Sarangi, A., & Singh, D. K. (2010). Spatial variability of groundwater depth and quality parameters in the national capital territory of Delhi. *Environmental Management, 45*, 640–650.

Demir, Y., Ersahim, S., Güler, M., Cemek, B., Günal, H., & Arslan, H. (2009). Spatial variability of depth and salinity of groundwater under irrigated ustifluvents in the Middle Black Sea Region of Turkey. *Environmental Monitoring Asscss, 158*, 279–294.

Di, H. J., & Cameron, K. C. (2002). Nitrate leaching in temperate agroecosystems: Sources, factors and mitigating strategies. *Nutrient Cycling in Agroecosystems, 46*, 237–256.

Di, H. J., Cameron, K. C., Bidwell, V. J., Morgan, M. J., & Hanson, C. (2005). A pilot regional scale model of land use impacts on groundwater quality. *Management of Environmental Quality, 16*, 220–234.

El Ayni, F., Cherif, S., Jrad, A., & Trabelsi-Ayadi, M. (2011). Impact of treated wastewater reuse on agriculture and aquifer recharge in a coastal area: Korba case study. *Water Resources Management, 25*, 2251–2265.

Evrendilek, F., & Ertekin, C. (2007). Statistical modeling of spatio-temporal variability in monthly average daily solar radiation over Turkey. *Sensors, 7*, 2763–2778.

ESRI. (2003). Using Arc GIS Geostatistical Analyst. Printed in the USA.

Gassama, N., Dia, A., & Violette, S. (2012). Origin of salinity in a multilayered aquifer with high salinization vulnerability. *Hydrological Processes, 26*, 168–188.

Farez, M. (2008). Effet de l'irrigation par les eaux uses traitées sur la variation des nitrates dans les eaux souterraines: Cas du perimeter irrigué de Bir Rommana (Nabeul). Master of Science. Tunis el Manar University.

Getis, A. (2007). Reflections on spatial autocorrelation. *Regional Science and Urban Economics, 37*, 491–496.

Goovaerts, P. (1999). Geostatistics in soil science: State-of-the-art and perspectives. *Geoderma, 89*, 1–45.

Goovaerts, P., AvRuskin, G., Meiliker, J., Slotnick, M., Jacquez, G., & Nriagu, J. (2005). Geostatistical modeling of the spatial variability of arsenic in groundwater of southeast Michigan. *Water Resources Research, 41*, 1–19.

Hanjra, M. A., Blackwell, J., Carr, G., Zhang, F., & Jackso, T. M. (2012). Wastewater irrigation and environmental health: Implications for water governance and public policy. *International Journal of Hygiene and Environmental Health, 215*, 255–269.

Isaaks, E. H., & Srivastava, R. M. (1989). *An introduction to applied geostatistics*. New York: Oxford University.

Johnson, T. D., & Belitz, K. (2009). Assigning land use to supply wells for statistical characterization of regional groundwater quality. *Journal of Hydrology, 370*, 100–108.

Juang, K. W., Liou, D. C., & Lee, D. Y. (2002). Site specific application based on the kriging fertilizer-phosphorus availability index of soils. *Journal of Environmental Quality, 31*, 1248–1255.

Karrou, J., Renard, P., & Tarhouni, J. (2010). Status of the Korba groundwater resources (Tunisia): Observations and three-dimensional modelling of seawater intrusion. *Hydrogeology Journal, 18*, 1173–1190.

Khelil, M. N., Rejeb, S., Trad, M., Hachicha, M., & Jozdane, O. (2009). Arrière effet des métaux lourds apportés par les eaux usées sur certaines cultures maraîchères. *Annales de l'INRGREF, 14*, 235–244.

Klay, S., Charef, A., Ayed, L., Houman, B., & Rezgui, F. (2010). Effect of irrigation with treated wastewater on geochemical properties (saltiness, C, N and heavy metals) of isohumic soils (Zaouit Sousse perimeter, Oriental Tunisia). *Desalination, 253*, 180–187.

Lalor, G. C., & Zhang, C. (2001). Multivariate outlier detection and remediation in geochemical databases. *The Science of the Total Environment, 281*, 99–109.

Li, Y. (2010). Can the spatial prediction of soil organic matter contents at various sampling scales be improved by using regression kriging with auxiliary information? *Geoderma, 159*, 63–75.

Lorenzen, G., Sprenger, C., Baudron, P., Gupta, D., & Pekdeger, A. (2011). Origin and dynamics of groundwater salinity in the alluvial plains of western Delhi and adjacent territories of Haryana State. *Hydrological_Processes, 26*, 2333–2345.

Louati, M., Khanfir, R., Alouini, A., El Echi, M., Frigui, L., & Marzouk, A. (2000). Guide pratique de gestion de la sécheresse en Tunisie. Rapport interne. Ministère de l'agriculture.

Mariez V. (2008). Impact de l'utilisation des eaux uses pour l'irrigation de parcelles cultivées sur la qualité microbiologique des en zone semi-aride (Tunisie). Insitiut Nationale de la Recherche Agronomique-France. Rapport de stage.

McLay, C. D. A., Dragten, R., Sparling, G., & Selvarajah, N. (2001). Predicting groundwater nitrate concentrations in a region of mixed agricultural land use: A comparison of three approaches. *Environmental Pollution, 115*, 191–204.

McGrath, D., & Zhang, C. (2003). Spatial distribution of soil organic carbon concentrations in grassland of Ireland. *Applied Geochemistry, 18*, 1629–1639.

Mohamed, M. A. A., Terao, H., Suzuki, R., Babiker, I. S., Otha, K., Kaori, K., et al. (2003). Natural denitrification in the Kakamigahara groundwater basin, Gifu prefecture, central Japan. *Science of the Total Environment, 307*, 191–201.

Moran, P. (1948). The interpretation of statistical maps. *Journal of the Royal Statistical Society, 10*, 243–251.

ONAS. (1993). Etude de factibilité d'assainissement 2001. Réutilisation des eaux usées épurées et des boues stabilisées des stations d'épurations. Office National d'Assainissement. Tunisia.

ONAS. (2008). Rapport annuel d'exploitation des stations d'épuration année 2008. Office National d'Assainissement. Tunisia; (unpublished).

ONAS. (2011). Rapport annuel 2010. [http://www.onas.nat.tn/Fr/upload/telechargement/telechargement99.pdf]. Last access, June 2012.

Prasannakumara*, V., Vijitha, H., Charuthaa, R., & Geetha, N. (2011). *Procedia Social and Behavioral Sciences, 21*, 317–325.

Sadeghi, A., Graff, C. D., Starr, J., Mccarty, G., Codling, E., & Sefton, K. (2006). Spatial variability of soil phosphorous levels before and after poultry litter application. *Soil Science, 171*, 850–857.

Salgos, M., Huertas, E., Weber, S., Dott, W., & Hollender, J. (2006). Wastewater reuse ad risk: Definition of key objectives. *Desalination, 187*, 29–40.

Serhal, H., Bernard, D., El Khattabi, J., Bastin-Lacherez, S., & Shahrour, I. (2009). Impact of fertilizer application and urban wastes on the quality of groundwater in the Cambrai Chalk aquifer. *Northern France. Environ Geol., 57*, 1579–1592.

Shapiro, S. S., Wilk, M. B., & Chen, H. J. (1968). A comparative study of various tests of normality. *Journal of the American Statistical Association, 63*, 1343–1372.

Sollitto, D., Romic, M., Castrignanò, A., Romic, D., & Bakic, H. (2010). Assessing heavy metal contamination in soils of the Zagreb region (Northwest Croatia) using multivariate geostatistics. *Catena, 80*, 182–194.

Spalding, R. F., Watts, D. G., Schepers, J. S., Burbach, M. E., Exner, M. E., Poreda, R. J., et al. (2001). Controlling nitrate leaching in irrigated agriculture. *Journal of Environmental Quality, 30*, 1184–1194.

Stigter, T. Y., Carvalho Dill, A. M. M., Ribeiro, L., & Reis, E. (2006). Impact of the shift from groundwater to surface water irrigation on aquifer dynamics and hydrochemistry in a semi-arid region in the south of Portugal. *Agric. Water Manage., 85*, 121–132.

Trangmar, B. B., Yost, R. S., & Uehara, G. (1985). Application of geostatistics to spatial studies of soil properties. *Advances in Agronomy, 38*, 45–94.

Tutmez, B., & Hatipolu, Z. (2010). Comparing two data driven interpolation methods for modelling nitrate distribution in aquifer. *Ecological Informatics., 5*, 311–315.

Van den Brink, C., Frapporti, G., Griffioen, G., & Zaadnoordijk, W. J. (2007). Statistical analysis of anthropogenic versus geochemical-controlled differences in groundwater composition in The Netherlands. *Journal of Hydrology, 336*, 470–480.

Varouchakis, E. A., Hristopulos, D. T., & Karatzas, G. P. (2012). Improving kriging of groundwater level data using non-linear normalizing transformations—A field application. *Hydrological Sciences Journal, 57*, 1404–1419.

Varouchakis, E. A., & Hristopulos, D. T. (2013a). Comparison of stochastic and deterministic methods for mapping groundwater level spatial variability in sparsely monitored basins. *Environmental Monitoring and Assessment, 185*, 1–19.

Varouchakis, E. A., & Hristopulos, D. T. (2013b). Improvement of groundwater level prediction in sparsely gauged basins using physical laws and local geographic features as auxiliary variables. *Advances in Water Resources, 52*, 34–49.

Webster, R., & Oliver, M. (2007). *Geostatistics for environmental scientists* (2nd ed.). West Sussex, England: John Wiley & Sons Ltd.

WHO. (2004). Drinking water quality guidelines. Volume 1: Recommendations. World Health Organization. Geneva (Suiza). [http://www.who.int/water_sanitation_health/dwq/gdwq3_es_fulll_lowsres.pdf]. Last access May 2012.

Yamamoto, J. K. (2005). Correcting the smoothing effect of ordinary kriging estimates. *Mathematical geology., 37*, 69–94.

Zghibi, A., Zouhri, L., & Tarhouni, J. (2011). Groundwater modelling and marine intrusion in the semi-arid systems (Cap-Bon, Tunisia). *Hydrological processes., 25*, 1822–1836.